Topics in Current Chemistry (2020) 378:20
https://doi.org/10.1007/s41061-020-0284-x

REVIEW

High-performance biosensing based on autonomous enzyme-free DNA circuits

Hong Wang[1] · Huimin Wang[1] · Itamar Willner[2] · Fuan Wang[1]

Received: 31 October 2019 / Accepted: 17 January 2020 / Published online: 3 February 2020

Abstract

Nucleic acids are considered not only extraordinary carriers of genetic information but also are perceived as the perfect elemental materials of molecular recognition and signal transduction/amplification for assembling programmable artificial reaction networks or circuits, which are similar to conventional electronic logic devices. Among these sophisticated DNA-based reaction networks, catalytic hairpin assembly (CHA), hybridization chain reaction (HCR), and DNAzyme represent the typical nonenzymatic amplification methods with high robustness and efficiency. Furthermore, their extensive hierarchically cascade integration into multi-layered autonomous DNA circuits establishes novel paradigms for constructing more different catalytic DNA nanostructures and for regenerating or replicating diverse molecular components with specific functions. Various DNA and inorganic nanoscaffolds have been used to realize the surface-confined DNA reaction networks with significant biomolecular sensing and signal-regulating functions in living cells. Especially, the specific aptamers and metal-ion-bridged duplex DNA nanostructures could extend their paradigms for detecting small molecules and proteins in even living entities. Herein, the varied enzyme-free DNA circuits are introduced in general with an extensive explanation of their underlying molecular reaction mechanisms. Challenges and outlook of the autonomous enzyme-free DNA circuits will also be discussed at the end of this chapter.

Keywords Catalytic hairpin assembly · Hybridization chain reaction · DNAzyme · DNA circuit · Imaging · Biosensor

Chapter 11 was originally published as Wang, H., Wang, H., Willner, I.·& Wang, F. Topics in Current Chemistry (2020) 378: 20. https://doi.org/10.1007/s41061-020-0284-x.

✉ Fuan Wang
fuanwang@whu.edu.cn

[1] College of Chemistry and Molecular Sciences, Wuhan University, Wuhan, People's Republic of China

[2] Institute of Chemistry, The Hebrew University of Jerusalem, Jerusalem, Israel

1 Introduction

In recent years, nucleic acids have substantially expanded their functions from natural bioinformation storage platforms to potent and designable tools for biosensing and bioengineering applications [1]. DNA represents the most powerful candidate for assembling artificial reaction networks for their intrinsic biocompatibility and programmability features. DNA reaction networks are composed of a series of successive strand displacement reactions and cascaded hybridization chain reactions, and they are especially appealing in investigating the signal pathways of more different cellular compartments, e.g., cytoplasm. As compared with the current artificial reaction networks, the advantage of DNA is overwhelmingly obvious for the following reasons. Firstly, DNA could be easily accommodated into different biological microenvironments without additionally complicating the information transmission between biological systems and electronic devices. Secondly, the directionality and programmability of DNA provides the most up-to-date powerful circuitry design and information storage based on the well-known Watson–Crick base-pairing interaction. Thirdly, more different functional DNAs, including aptamers and DNAzymes with their molecular recognition and signal transmission capabilities, could be facilely integrated into the present DNA-based artificial reaction networks. This allows the sensitive and selective sequence-specific analysis of nucleic acids, small molecules, and proteins, which is of great vitality for pathogen identification [2], medical diagnosis [3, 4], and environmental and food safety monitoring [5]. As a traditional nucleic acid amplification method, the polymerase chain reaction (PCR) shows a powerful capability to sensitively detect trace amounts of nucleic acids and other analytes [6, 7]. However, to guarantee the successful initiation of an efficient amplification, PCR needs complex and precise thermocycling procedures with specific polymerases, which may limit its applications in the detection of non-nucleic acid targets as well as in thermosensitive environments. As alternative tools, some isothermal signal amplification methods have thus been developed with more convenient and satisfying amplification capacity, including loop-mediated isothermal amplification (LAMP) [8], rolling circle amplification (RCA) [9, 10], as well as strand displacement amplification (SDA) [11, 12]. While these amplification methods are still bothered by the fragile biological enzymes. Enzyme-free isothermal detection methods are increasingly developed as alternative strategies for overcoming these limitations. The nonenzymatic DNA reaction networks provide the ideal candidate to fulfill these different requirements based on the versatile design out of protein enzyme. Then how to improve these nucleic acid amplification technologies that can compete with the current gold-standard enzyme-mediated amplification methods? Here, the topic of autonomous enzyme-free DNA reaction circuits will be discussed in this chapter by addressing the construction of different kinds of DNA reaction schemes and their effective integration with an adequate discussion of their potential applications.

2 Enzyme-Free DNA Circuit

Nucleic acid reaction networks have attracted increasing attention in the fields of analytical chemistry and biochemistry, and have been explored for sensitive detection of various target molecules. Enzyme-free signal amplification methods are especially appealing for the development of more robust and low-cost point-of-care diagnostics [13]. Among these different enzyme-free DNA reaction circuits, catalyzed hairpin assembly (CHA) [14] and hybridization chain reaction (HCR) [15] are emerging as typical amplification strategies that depend only on autonomous hybridization and strand-displacement reactions to achieve efficient signal amplifications [16]. Figure 1 exemplifies the well-known toehold-mediated strand displacement [17]. During this process, the initial DNA duplex is elongated with an exposed single-stranded domain, namely toehold that can hybridize partially with the input DNA primer. Then the sequential branch migration proceeds, and the input gradually displaces one primer that is partially (or fully) complemented to the other primer of the duplex, yielding a new and more stable DNA duplex structure. As shown in Fig. 1a, the primers P1 and P2 are connected by the hybridization of a–a* (domain x corresponds to a Watson–Crick base-pairing with x*.) that is elongated with a toehold sequence a_t. The DNA complex P1/P2 hybridizes with the input DNA P3 by toehold binding of a_t*–a_t, after which the a*–a-mediated sequential branch migration leads to the ultimate assembly of P1/P3 product with the simultaneous generation of P2 strand. Interestingly, the kinetics (rate constant) of these strand-displacement reactions varied with the base numbers and species of toehold domains (Fig. 1b), and the G–C-rich toehold leads to a higher strand displacement reaction rate than that of the A–T counterpart.

Based on this mechanism, various research has been carried out to address the strand-displacement process and to extend their broader applications. Among these different works, CHA and HCR have been well developed and have attracted more

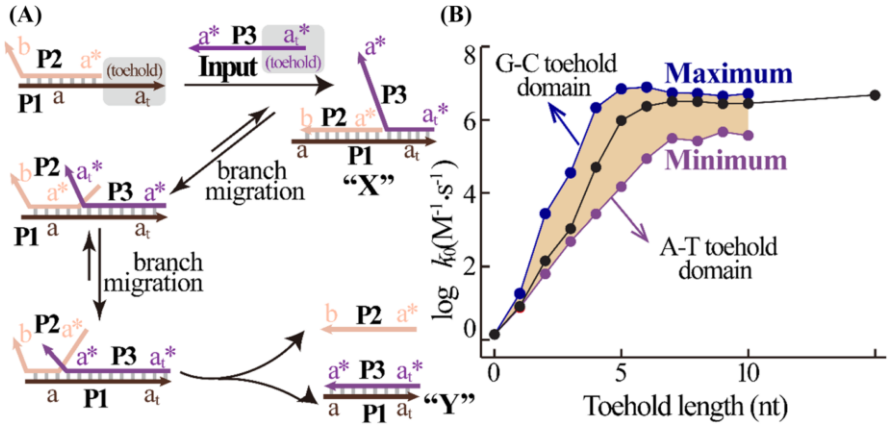

Fig. 1 **a** Schematic illustration of DNA strand-displacement principle. **b** Kinetics models of DNA strand-displacement reaction that were affected by the number and species of bases in the toehold domain. Reprinted with permission from Ref. [17]. Copyright 2009 American Chemical Society

attention for their isothermal and autonomous hybridization reaction properties. In a typical CHA process, the initiator acts as a special key to cyclically open their corresponding hairpin locks without consuming the input strand itself. CHA mediates the target-catalyzed hybridization and strand-displacement of hairpins for assembling numerous dsDNA products, which are especially useful in amplifying and transducing the input DNA at the terminus of nucleic acid amplifications. Indeed, CHA is facilely conjugated with other amplification procedures to achieve an improved sensing performance. As for the HCR, the input primer promotes the autonomous cascade cross-hybridization of hairpin reactants, yielding long nicked dsDNA copolymers through an easy and programmable operation. Also, the generated long dsDNA nanowire products are not only encoded with various functional DNA sequences but are also utilized as powerful nanocarriers for accommodating small guest molecules [18]. Meanwhile, DNAzymes are emerged with fascinating catalytic functions of protein enzymes that can catalyze various biological and chemical reactions, including DNA ligation and cleavage. These enzyme-mimicking functionalities with multiple turnover rates allow DNAzymes to be ideal candidates for high-performance signal amplification applications. All of these enzyme-free DNA circuits have prominent and modular amplification features—that is, their signal gain performance could be improved by integrating with other amplification methods in more extended application fields. These nonenzymatic amplification strategies have been used to detect various important analytes (nucleic acids [19, 20], proteins [21], small molecules [22], and metal ions [23]) with different transduction approaches, such as fluorescence [24, 25], colorimetry [26], chemiluminescence (CL) [27], and electrochemical approaches [28].

2.1 Catalytic Hairpin Assembly (CHA)

The analyte-activated isothermal autonomous catalytic hairpin assembly (CHA) was initially proposed by Pierce et al. [14]. It provides a versatile free-energy-driven amplification procedure to stimulate the catalytic generation of stable linear or branched duplex DNA nanostructures. The mechanism of CHA is presented in Fig. 2a. A characteristic CHA reaction consists of two hairpins, H_A and H_B. The sequence a_t–a of H_A is complementary to domain a*–a_t* of trigger T, and hairpin H_B is designed to hybridize with H_A from b_t*. T opens hairpin H_A to generate the DNA assembly "I" based on toehold-mediated displacement of sequence a*–a_t*. The released domain b–b_t of H_A hybridizes with hairpin H_B, generating an intermediate structure "II". The newly released H_B initiates the branch migration procedure and gradually stimulates the strand displacement of T to form numerous dsDNA product "III". The regenerated trigger strand allows the continuous activation of CHA circuit that stimulates the successive hybridizations between hairpins H_A and H_B. Similarly, more different hairpins can be assembled by CHA to generate a "Y-shaped" model with three hairpin reactants or "X-shaped" model with four hairpin reactants.

The trigger-induced CHA-mediated cross-opening of nucleic acid hairpins could also enhance the complexities of DNA nanostructures. As shown in Fig. 2b, the cascaded cross-opening of three hairpins leads to the formation of a three-arm branched

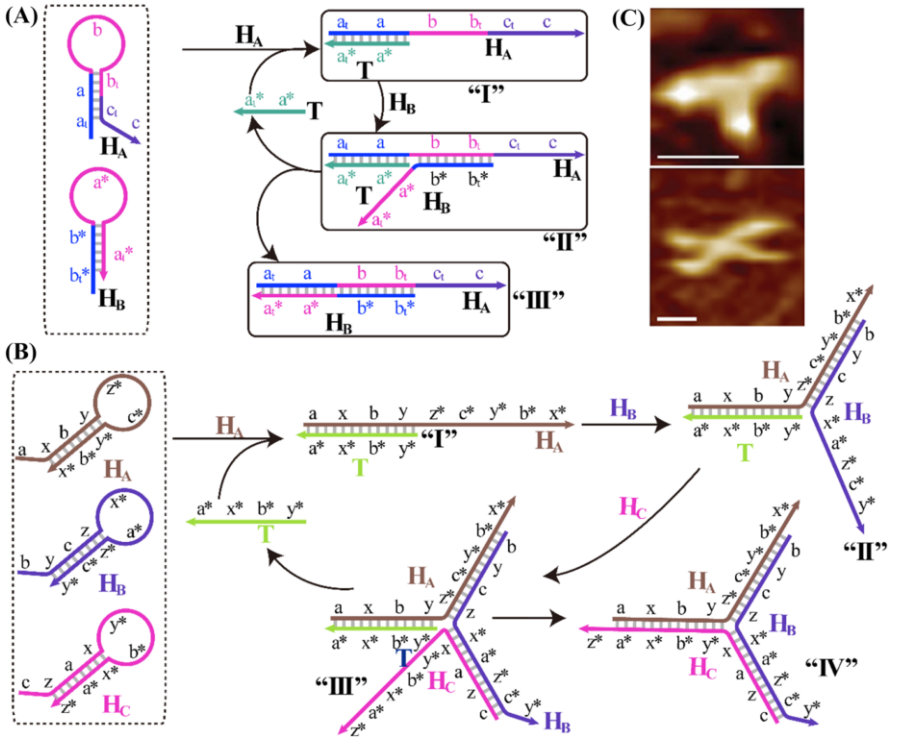

Fig. 2 Schematic illustration of conventional CHA. **a** CHA-assembled linear dsDNA nanostructure, which is induced by trigger-catalyzed assembly of hairpins H_A and H_B. **b** CHA-assembled Y-shaped DNA nanostructure that is generated by cross-opening of hairpins H_A, H_B, and H_C. **c** AFM images of the CHA-assembly of "Y-shaped" (upper AFM image) and "X-shaped" (lower AFM image) dsDNA nanostructures, respectively. Scale bar indicates 10 nm. Reprinted with permission from Ref. [14]. Copyright 2008 Nature Publishing Group

junction structure. The initiator T hybridizes with hairpin H_A to generate dsDNA product "I", and the toehold of "I" opens H_B to generate structure "II". The exposed toehold in "II" opens H_C to form an intermediate structure "III". The newly released strand of H_C initiates the branch migration and displaces T to form the three-arm branched junction structure "IV". The released initiator subsequently stimulates the successive hybridizations among hairpins H_A, H_B, and H_C to generate "Y-shaped" DNA nanostructures. Similarly, the four-arm branched junction structure could be programmed through the catalytic self-assembly of four hairpins, as demonstrated in Fig. 2c. The autonomous regeneration of trigger with the cross-opening hairpin-mediated hybridization method represents an isothermal enzyme-free amplification method for the analysis of trigger DNA.

The as-demonstrated CHA system can be extended as a powerful sensing platform for analyzing nucleic acids and more different analytes via fluorescence transduction [29]. In Fig. 3a, trigger T hybridizes with hairpin H_{CP} to generate the actual initiator T-H_{CP} with a newly exposed toehold sequence (light blue), and

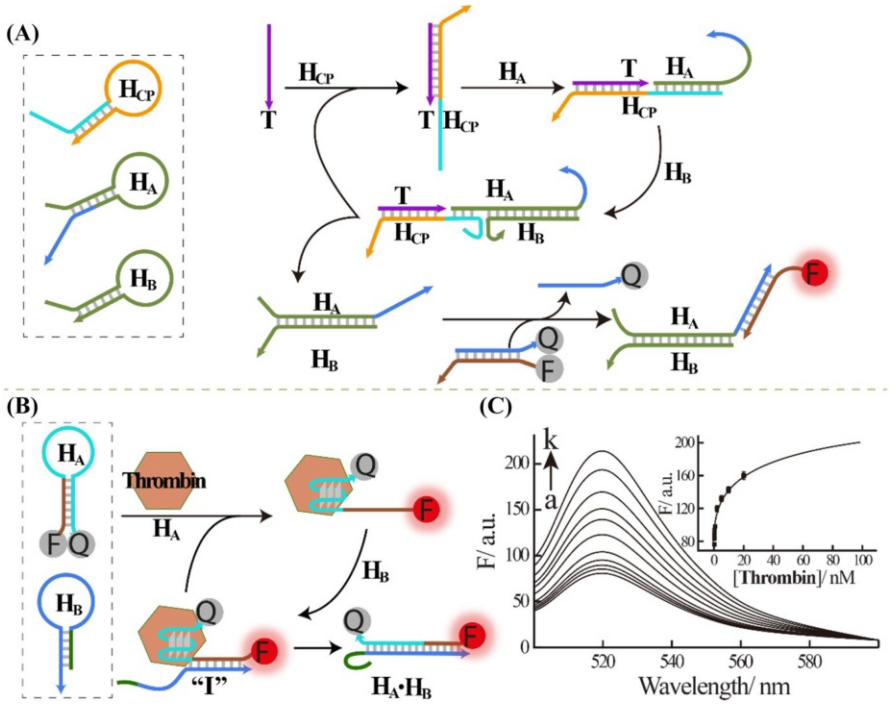

Fig. 3 **a** Schematic illustration of an isothermal autonomous CHA amplifier for analyzing target DNA with the aid of an auxiliary sensing module H_{CP}. **b** Schematic illustration of the analysis of thrombin based on the CHA-mediated transduction of an aptamer recognition module. **c** Fluorescence spectrum of the CHA-amplified thrombin detection system by incubating with different concentrations of thrombin: a–k: 0, $2.0\times g\ 10^{-11}$, 5.0×10^{-11}, 2.0×10^{-10}, 5.0×10^{-10}, 2.0×10^{-9}, 5.0×10^{-9}, 1.0×10^{-8}, 2.0×10^{-8}, 5.0×10^{-8}, and 1.0×10^{-7} M. (Inset) Derived calibration curve. Reprinted with permission from Ref. [30]. Copyright 2012 Elsevier

then the T-H_{CP} initiator catalyzes the cross-opening of H_A and H_B to implement the CHA reaction, yielding a duplex H_A–H_B with a single-strand domain (dark blue) that could displace a fluorophore/quencher-modified duplex and generate fluorescence readout for detecting DNA targets [30]. Apart from DNA detection, CHA could also be applied for protein detection with the specifically designed aptamer that was encoded into one of these two hairpin reactants (H_A and H_B), Fig. 3b. Here, H_A contains a thrombin–aptamer sequence in the loop region and is attached with a fluorophore/quencher pair on each end. In the presence of thrombin, H_A is opened to form the thrombin–aptamer complex with a toehold (brown), which then opens H_B to generate an intermediate structure "I". The exposed toehold of H_B competitively binds the aptamer region associated with thrombin and releases the thrombin analyte for continuously triggering the CHA system. The formation of H_A-H_B leads the efficient separation of fluorophore and quencher, and generates high fluorescence signal for analyzing thrombin down to 20 pM (Fig. 3c).

Apart from the programmed catalytic assembly of different DNA nanostructures, the CHA reaction could be facilely engineered as a stochastic DNA walker that utilizes hybridization reactions to traverse a microparticle surface. Figure 4a exemplifies the initiator-catalyzed successive cross-opening of surface-immobilized H_1 and FAM-functionalized H_2 on microparticles [31]. The catalyst DNA can open the surface-bound H_1 through toehold-mediated strand-displacement reaction. Then, a newly released tether of H_1 hybridizes to the toehold of FAM-modified H_2 for initiating a branch migration reaction, resulting in the generation of an intermediate structure consisting of H_1, H_2, and the catalyst. Along with the strand displacement process, the catalyst DNA is displaced from the duplex structure of H_1–H_2. The regenerate catalyst then continuously participates in the nearby CHA reaction cycle. Through the CHA process, the nanoscale movements of the walker (catalyst) lead to the immobilization of fluorescent strands on the surface of the microparticle.

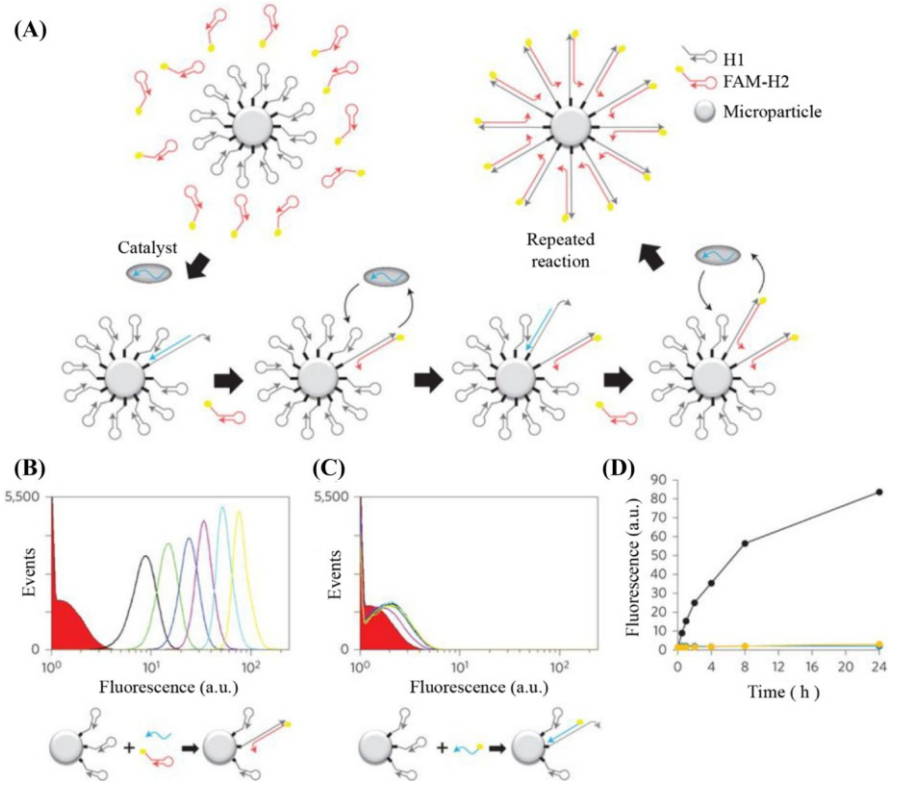

Fig. 4 **a** Schematic illustration of the microparticle-confined CHA based on the catalytic hybridization reaction between surface-anchored H_1 and non-anchored FAM-modified H_2. **b** Flow cytometry characterization of the microparticle-confined CHA over different time intervals (0, 0.5, 1, 2, 4, 8, 24 h, from left to right). **c** Flow cytometry characterization of the negative CHA control experiment without the involvement of H_2. **d** Summary of the mean fluorescence intensity from the flow cytometry assay over time (black for catalytic system; blue and yellow for non-catalytic and no-catalyst controls, respectively). Reprinted with permission from Ref. [31]. Copyright 2016 Nature Publishing Group

An obvious fluorescence change over different time intervals has demonstrated the successful capture of FAM-H_2 on microparticles through the as-suggested CHA process (Fig. 4b). The H_2-absent negative control experiment was carried out with substantially lower fluorescence readout and thus exemplified the amplification performance of CHA (Fig. 4c). This signal difference could be easily observed from the summarized flow cytometry assay, as shown in Fig. 4d. The walking system offers new insights into the analytical and diagnostic applications, as well as biomaterials development.

By using the underlying nanoparticles as nanocarriers, the CHA system could also be applied towards sensitive detection of intracellular RNA, e.g., manganese superoxide dismutase (MnSOD) mRNA in living cells [32]. Subsequently, other functional nanostructures, e.g., tetrahedron DNA, are also supplemented versatile tools to deliver DNA primers into living cells, considering that the homologous DNA could be assembled into suitable size and shape for delivering DNA probes. An entropy-driven three-dimensional DNA amplifier (EDTD) has been constructed for delivering DNA probes into living cells where a specific intracellular mRNA analyte triggers the EDTD-involvement CHA process [33]. As illustrated in Fig. 5a, the first module of EDTD corresponds to an entropy tetrahedron (ET) module that is constructed with six DNA primers and elongated an important dsDNA toehold. Here, the quencher-modified P5 and the fluorophore-modified P6 are assembled together with no fluorescence readout. The other key module of EDTD is the fuel tetrahedron (FT) module (Fig. 5b). Similar to ET, the FT uses four DNA primers to construct the same tetrahedral backbone. Different from P4, here part of P7 toehold acts as fuel sequence (yellow) in the CHA process. The tetrahedron amplifier could be quickly activated by target mRNA which hybridizes with the exposed region 4*

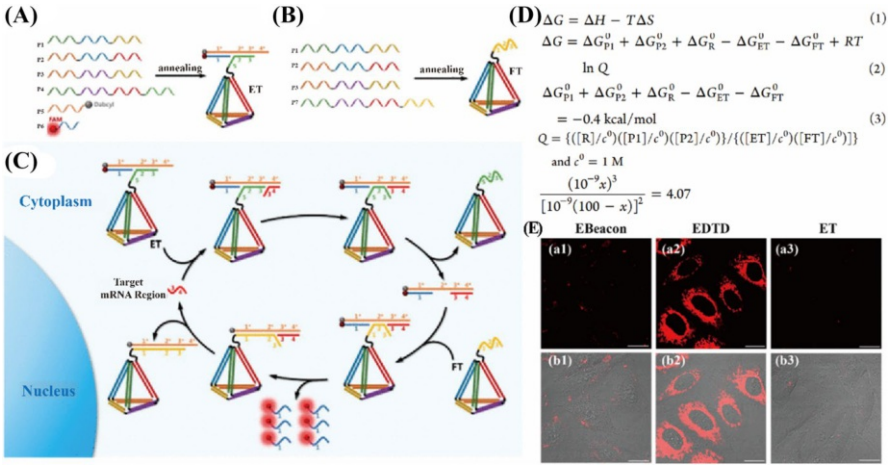

Fig. 5 Schematic illustration of the assembly of the entropy tetrahedron (ET) module (**a**), the fuel tetrahedron (FT) module (**b**), and the EDTD principle in living cells (**c**). **d** Theoretical simulation of the EDTD reaction. **e** EDTD-mediated intracellular imaging of TK1 mRNA in HepG2 cells that were treated with different systems. Scale bar 20 μm. Reprinted with permission from Ref. [33]. Copyright 2018 American Chemical Society

of ET to initiate the toehold-mediated strand displacement, resulting in an immediate T–P5–P6 product (Fig. 5c). The as-achieved T–P5–P6 structure binds to the exposed domain 2* of FT to release target mRNA and P6 with the formation of a waste tetrahedron FT-P5 product. The regenerate mRNA and P6 can take part in the next cycle of CHA reaction to realize an effective signal amplification. Therefore, the fluorescence of P6 can directly reflect the amount of intracellular mRNA. Different from the cross-opening of convenient CHA reaction, this new strategy is free from hairpin reactants and is driven by entropy as demonstrated by theoretical simulations (Fig. 5d). Benefiting from this special structure and the exclusive driving force, this DNA nanostructure could be operated in living cells for a high-performance mRNA detection (Fig. 5e). This entropy-driven 3D DNA nano-amplifier might provide a more reliable sensing platform for living entities.

2.2 Hybridization Chain Reaction (HCR)

Another characteristic isothermal non-enzymatic nucleic acid reaction, hybridization chain reactions (HCR), is achieved by successive cross-opening of two hairpins to assemble dsDNA copolymeric nanowires [15]. As shown in Fig. 6a, H_1 consists of the programmed sequences a–b and c–b*, which are complementary to the sequence b*–a* of initiator I and b–c* of H_2, respectively. The rest sequence of H_2 corresponds to domain b*–a*, an analog sequence of I, which can subsequently hybridize to domain a–b of H_1. These hairpins stay in a kinetically trapped situation without initiator. Based on the toehold-mediated displacement process, initiator

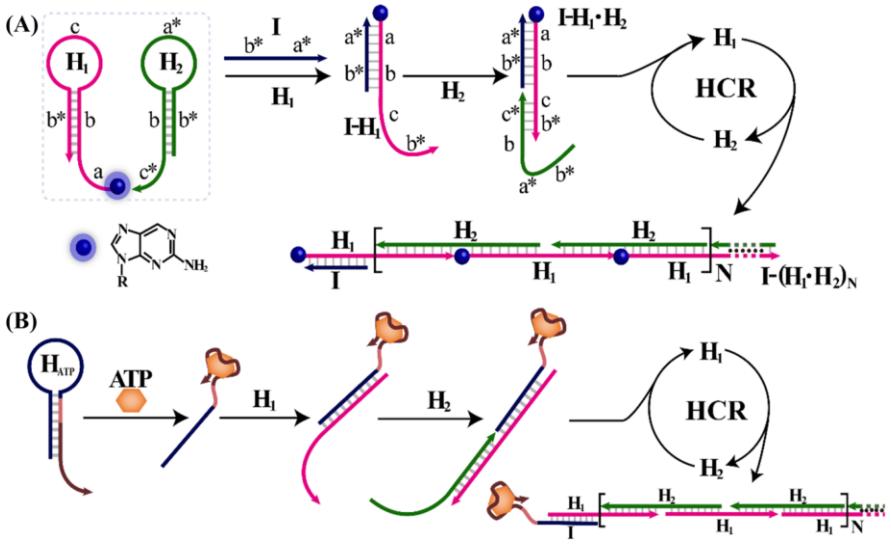

Fig. 6 **a** Schematic illustration of the HCR circuit where the initiator I triggers the autonomous cross-opening of H_1 and H_2 to generate dsDNA nanowires. **b** Amplified ATP detection by integrating HCR amplification with functional hairpin H_{ATP}

I opens hairpin H_1 to generate I·H_1 duplex. The released domain c–b* in I·H_1 opens H_2 to form an immediate product I·H_1·H_2 of which the exposed sequence b*–a* initiates the following new round of hybridization cycle, resulting in the generation of long dsDNA polymeric nanowires. Here, H_1 is functionalized with 2-amino purine, which shows high fluorescence in the single-stranded configuration of the hairpin structure, while it is quenched by stacking in the duplex DNA nanowire structure. More importantly, the HCR circuit could be served as an easily adapted amplifier for extensive sensing applications, e.g., aptasensors (Fig. 6b).

The HCR system could also be considered as a more versatile sensing platform when the HCR reactants H_1 and H_2 were labeled with two pyrene moieties on each end (Fig. 7a) [34]. Without target DNA, both hairpins are in the closed form, and the two pyrene moieties are separated far away from each other through the sticky end, leading to the observation of the monomer emission spectra. Target DNA can open H_1 through a strand-displacement reaction. The newly released toehold of H_1

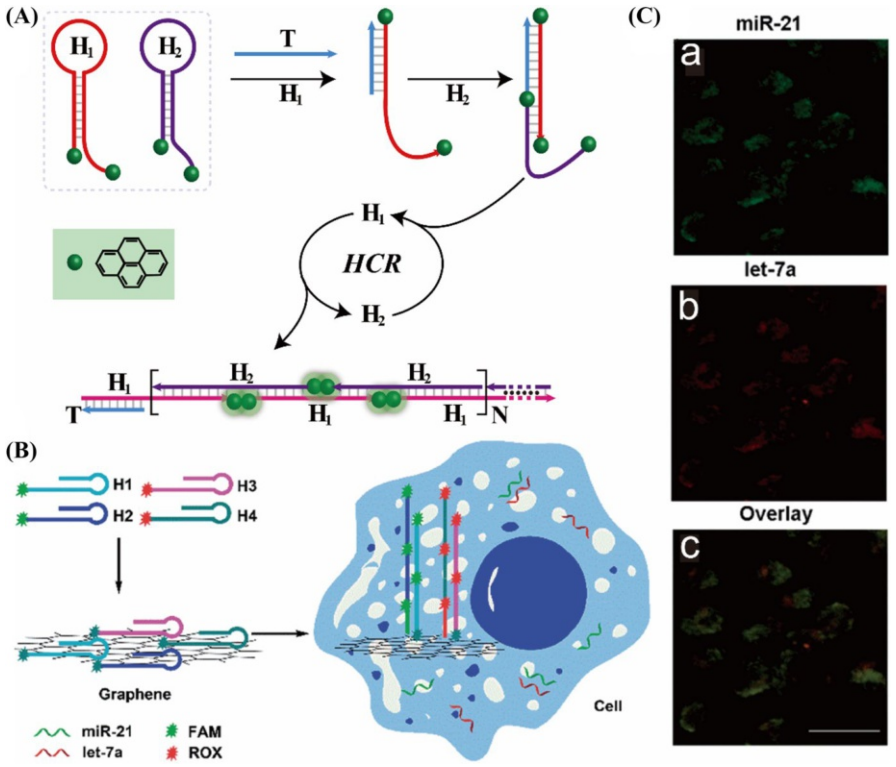

Fig. 7 **a** The autonomous HCR system based on the target-induced cross-hybridization of H_1 and H_2 that were functionalized with pyrene units in two ends, resulting in the generation of long dsDNA nanowires with exciplex emission of pyrene. **b** Schematic illustration of the intracellular multicolor miRNA imaging based on the HCR reaction on graphene oxide (GO). **c** Two-color confocal fluorescence imaging of miR-21 and let-7a analytes in MCF-7 cells. The scale bar indicates 50 μm. Reprinted with permission from Ref. [36]. Copyright 2017 Royal Society of Chemistry

nucleates at the tether end of H_2 and opens H_2 to expose another target analog. Thus, the target can propagate a successive cross-opening of two hairpins to yield long dsDNA nanowires. In this HCR product, the pyrene moieties are brought into close proximity, thus generating numerous pyrene excimers with an emission at approximately 485 nm. Therefore, the target can be sensitively detected by the varied emissions of pyrene monomers and the corresponding excimers.

Two-dimensional nanomaterials, including graphene oxide (GO) [35], molybdenum disulfide (MoS_2), and manganese dioxide (MnO_2), could also be integrated with HCR amplifier for intracellular mRNA imaging, originating from their excellent capability of ssDNA adsorbing and fluorescence quenching. Figure 7b exemplified the simultaneous detection of two intracellular miRNAs by using GO-supported HCR circuit [36]. Here, H_1 and H_2 were functionalized with fluorophore FAM for miR-21 detection while H_3 and H_4 were modified with fluorophore ROX for let-7a detection. These hairpins were physically absorbed on the surface of GO through noncovalent π–π stacking interaction and all fluorophores were efficiently quenched. These hairpin probes were transported into living cells by GO via a non-destructive clathrin-mediated endocytosis process. Then the miR-21 target could initiate the successive hybridization between H_1 and H_2, yielding long dsDNA $(H_1/H_2)_n$ nanowires. These nanowires were then detached from the surface of GO with fluorescence recovery of FAM, which is originated from the weak interaction between dsDNA and GO. Similarly, the let-7a analyte could trigger the sequential hybridization of H_3 and H_4 for obtaining a remarkable higher fluorescence of ROX. The amplified green and red fluorescence signal represented the corresponding miRNAs in living cells, and thus providing a novel tool for sensitive intracellular imaging of multiple biomarkers (Fig. 7c).

Besides graphene oxide, gold nanoparticles (AuNPs) could also be utilized for transducing the HCR system via a colorimetric or fluorescent bioassay. Figure 8a illustrates the colorimetric detection system based on AuNPs transduction of HCR system consisting of two hairpins H_1 and H_2 [37]. Domains I and II of H_1 are designed to be complementary to domains I′ and II′ of H_2. Without target, the ssDNA tethers of HCR hairpins are absorbed on the surface of AuNPs, and thus avoid the salt-induced aggregation of AuNPs. The introduced target can hybridize with domain I of H_1 and open H_1 through strand displacement reaction (step 1). The newly exposed tether II of H_1 then hybridizes to domain II′ of H_2 and opens H_2 (step 2). The as-released domain I′ is encoded with the same sequence of target for triggering the efficient opening of H_1 (step 3). With the repeat operation of steps 2 and 3, the sequential hybridization of H_1 and H_2 leads to the efficient assembly of long dsDNA nanowires. Under this circumstance, these as-achieved nanowires are detached from the AuNPs, resulting in the aggregation of AuNPs under high-salt concentrations with immediate color transition. This method achieves a simple yet convenient colorimetric detection of DNA and could sensitively and selectively discriminate single base-pair mismatches of the target (Fig. 8a inset).

For HCR transduction, AuNPs were not only acting as colorimetric transduction agent, but were also considered as a versatile fluorescence quencher [38]. The combination of AuNPs with HCR circuit has also been applied for intracellular mRNA imaging. The target survivin mRNA is known to be overexpressed in

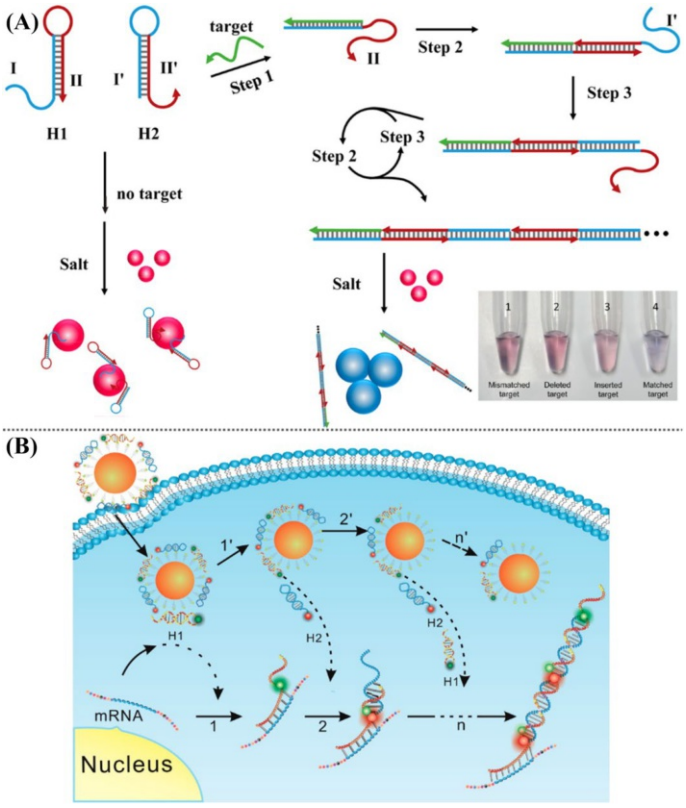

Fig. 8 **a** Schematic illustration of the colorimetric detection of DNA target through AuNPs-mediated transduction of HCR amplifier. Inset shows the corresponding photographs of AuNPs solutions that were introduced with different reactants. Reprinted with permission from Ref. [37]. Copyright 2013 American Chemical Society. **b** Scheme of the fluorescent detection of mRNA target using AuNPs-supported HCR amplification. Reprinted with permission from Ref. [39]. Copyright 2015 American Chemical Society

most cancer cells [39]. In Fig. 8b, two hairpin reactants H_1 and H_2 are designed to recognize and amplify the target mRNA. Here, H_1 and H_2 are functionalized with a fluorescence donor (FAM) and a fluorescence acceptor (TMR), respectively, and are steadily assembled on the surface of cationic peptide-coated AuNPs. These fluorescence signals are thus effectively quenched by AuNPs. The survivin mRNA opens hairpin H_1 with the exposure of an ssDNA tether. This tether sequence then hybridizes with hairpin H_2 and releases the same sequence of target. Then the alternative hybridization of H_1 and H_2 generates dsDNA nanowires with rigid conformation, resulting in the dissociation of these HCR nanowires from the surface of AuNPs. The dissociated product brings two fluorophores FAM and TMR into close proximity for generating an efficient Förster resonance energy transfer (FRET) signal. The gold particles-DNA nanoassembly enables high performance to deliver into living cells and to quench the DNA probes, thus offering high sensitivity and specificity for intracellular mRNA imaging. The

nanoassembly might provide a novel strategy for low-abundance biomolecule detection and regulation in cell biology studies.

The confined HCR reaction on AuNPs could similarly be extended to DNA nanostructures, e.g., rolling circle polymerized one-dimensional RCA nanowires. This DNA-confined HCR system is proposed as a powerful tool for realizing intracellular sensing applications (Fig. 9a) [40]. Based on an accelerated HCR system on the RCA track product, the DNA "nano string light" (DNSL) achieved high-performance intracellular mRNA imaging. This system was designed by interval immobilizing functional hairpins H_1 and H_2 on RCA-produced DNA nanowires. The fluorophore/quencher-modified hairpin H_1 was conjugated with folic acid (FA) for targeting HeLa cells. The intracellular survivin mRNA initiates the cascade cross-opening of the alternatively arranged H_1 and H_2 along the DNA nanowire, which could enhance the fluorescence of DNSL (Fig. 9b). In comparison with the non-confined catalytic amplification and successive DNA hybridization, the DNSL includes

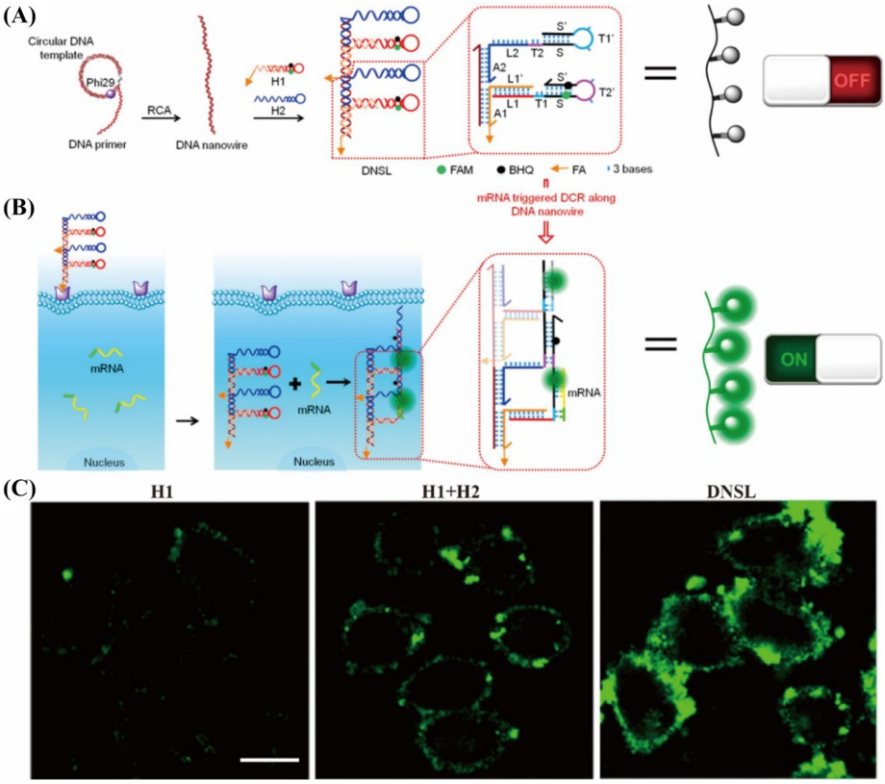

Fig. 9 Schematic illustration of the one-dimensional DNA scaffold-confined HCR reaction through the alternative arrangement of hairpins H_1 and H_2 on the RCA-produced nanowire. **a** DNSL synthesis procedure and **b** the targeting delivery of DNSL into living cells for imaging target mRNA. **c** Confocal images of HeLa cells that were treated with H_1, mixture of H_1 and H_2, and DNSL, respectively. Scale bar 20 μm. Reprinted with permission from Ref. [40]. Copyright 2018 American Chemical Society

numerous H_1 and H_2 that were alternately arranged with designed space, to accelerate hybridization reaction and strand-displacement with enhanced sensing performance. The biocompatible DNSL further facilitated the efficient delivery of HCR probes into living cells (Fig. 9c). It thus introduces a potential intracellular mRNA imaging platform for various disease diagnostics and therapies.

2.3 DNAzyme

DNAzymes are referred to as catalytic ssDNAs that are obtained via the in vitro selection. They usually require indispensable cofactors for executing an efficient catalytic DNA or RNA cleavage, DNA hydrolyzation, DNA ligation, and so on. One of the most commonly used DNAzymes is the metal ion-dependent RNA-cleaving DNAzyme, which requires the involvement of metal ion cofactors, such as Mg^{2+} [41], Cu^{2+} [42], Ni^{2+} [43], Hg^{2+} [44], Zn^{2+} [45], Pb^{2+} [46], and so on. The DNAzyme-based biocatalysis reactions have been extensively described in a series of review articles [47, 48]. As shown in Fig. 10a, the DNAzyme (blue strand) can specifically bind to the riboadenine (rA, yellow)-containing DNA substrate (purple strand) through Watson–Crick base pairing hybridization. The DNAzyme folds into the catalytic active structure with metal ions for cleaving substrate at "rA" site, releasing two fragments of the cleaved substrate. Here, the cleavage of RNA

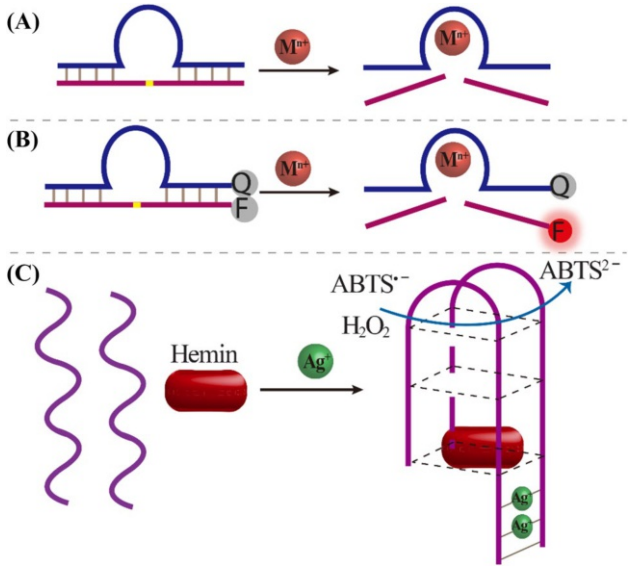

Fig. 10 **a** Schematic illustration of the DNAzyme-mediated RNA-cleavage with the aid of indispensable cofactors. **b** The design of fluorescent DNAzyme biosensors based on the fluorophore/quencher-modified DNAzyme and substrate. Reprinted with permission from Ref. [49]. Copyright 2017 American Chemical Society. **c** The specific Ag^+-involved assembly of cytosine-Ag^+-cytosine bridges for constructing hemin/G-quadruplex HRP-mimicking DNAzyme. Reprinted with permission from Ref. [52]. Copyright 2009 American Chemical Society

is mostly initiated by the attacking of 2′-OH group to the scissile phosphate. The released DNAzyme then moves to the cyclic cleavage of another substrate, thus achieving the amplified catalytic process. The substrate could be labeled with a F/Q pair for transducing the DNAzyme reaction process [49]. Figure 10b shows that the DNAzyme catalytically cleaves the FAM-labeled substrate with metal ion cofactors. The cleaved substrate fragments detached from the quencher-functionalized DNAzyme, resulting in the recovery of FAM fluorescence. Another widely used DNAzyme is the hemin/G-quadruplex horseradish peroxidase (HRP)-mimicking DNAzyme, which could mimic the catalytic functions of peroxidase for catalyzing the oxidation of ABTS or TMB with color changes, and the chemiluminescence of luminol with H_2O_2 [50, 51]. Since the cytosine–cytosine (C–C) gap of dsDNA can specifically capture Ag^+ ions to generate C–Ag^+–C bridge, a DNA-based Ag^+ sensor was then constructed [52]. Figure 10c depicts the hemin/G-quadruplex DNAzyme-mediated colorimetric detection of Ag^+ ions. Without Ag^+, these hemin/G-quadruplex strands are separated with each other with no DNAzyme activity. The Ag^+ ions can initiate the generation of C–Ag^+–C base pairs for assembling hemin/G-quadruplex DNAzyme. The as-achieved DNAzyme can catalyze the ABTS-H_2O_2 reaction and give rise to a colorimetric assay. This Ag^+-mediated DNAzyme switch system could be used for sensitive detection of Ag^+ with a detection limit of 2.5 nM.

Since the surface plasmon resonance absorption of AuNPs is affected by their size and distance, AuNPs are widely used in assembling various colorimetric sensors. This property is especially appealing for producing DNAzyme biosensors via the DNAzyme-conjugated AuNPs [53]. As shown in Fig. 11a, the AuNPs were modified with DNAzyme/substrate strands through Au–S bond. The DNAzyme-hybridized substrate was elongated to capture AuNPs, leading to the aggregation of AuNPs with blue color in solution. In the presence of Pb^{2+} cofactor, the DNAzyme was activated to cleave the substrate and led to the dissociation of gold nanoassembly with red color of the dispersed AuNPs. Not only metal ion cofactors, but other factors could also be considered as the specific analytes for their influence on the compact DNAzyme structure. With the help of AuNPs and aptamer-involved recognitions and activations, an amplified aptazyme–AuNPs biosensor was assembled for intracellular ATP detection [54]. Here, the aptazyme is designed with two major regions: ATP aptamer-recognition domain and DNAzyme transduction region. As shown in Fig. 11b, the ATP aptazyme and its substrate are both immobilized on AuNPs. Meanwhile, the ATP aptazyme is labeled with a quencher (BHQ-2) unit and the substrate is labeled with a fluorophore unit. In that case, the fluorophore would be effectively quenched by AuNPs and BHQ-2. Thus, the ATP aptazyme sensors are catalytic inactive without fluorescence readout. The ATP could specifically combine with aptazyme and favor the assembly of DNAzyme microenvironment for activating the cleavage reaction of DNAzyme substrate. After cleavage, the fluorophore-labeled DNA fragment is separated from the substrate strand and moves far from the quencher units, thus yielding a high fluorescence signal. The AuNPs surface-confined DNAzyme reaction leads to an efficient DNAzyme reaction as mentioned before. Thus, the free aptazyme keeps active to hybridize with other substrate strands on AuNPs for new cycles of DNAzyme cleavages, resulting in highly sensitive ATP

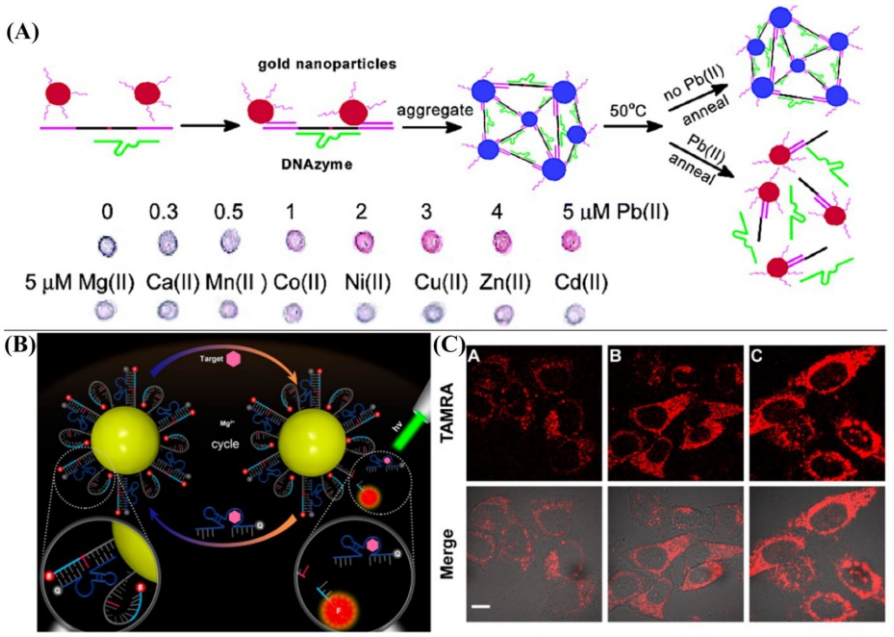

Fig. 11 **a** The colorimetric assay of lead ions based on the integration of DNAzyme biocatalysis with AuNPs labels. Reprinted with permission from Ref. [53]. Copyright 2003 American Chemical Society. **b** Schematic illustration of the AuNPs-confined aptazyme sensing platform for ATP assay. **c** Intracellular imaging of ATP by AuNPs-confined aptazyme reaction in HeLa cells that were treated with different systems: A, 10 μg/ml oligomycin and 5 mM 2-deoxy-D-glucose; B, intact control; C, 5 mM Ca^{2+}. Scale bar 10 μm. Reprinted with permission from Ref. [54]. Copyright 2016 American Chemical Society

detecting performance. Moreover, this strategy can further be applied for intracellular imaging of various targets in living cells (Fig. 11c). Similarly, based on the remarkable affinity difference between GO and ssDNA, the GO surface-confined DNAzyme has also been introduced for selective and amplified Pb^{2+} detection [55].

Apart from AuNPs integration, DNAzymes can also be applied to cascade with the endonucleases, which could realize a more sensitive enzymatic recycling cleavage strategy. The molecular recognition element was facilely integrated with a signal reporter element with improved sensitivity. As shown in Fig. 12a, the dual loop hairpin H_{lp} is composed of DNAzyme and substrate that were connected by a poly-T sequence. In the presence of L-histidine, the intramolecular cleavage reaction releases a trigger sequence T. Then the reporter MB is opened by trigger T to form the double-stranded recognition site for Nicking enzyme, realizing the second cycle of cleavage. The cascade DNAzyme-Nicking enzyme system undergoes sequential and successive cleavage of MB probe, providing a high fluorescence readout (Fig. 12b). This cascade-catalytic sensing strategy affords a sensitive L-histidine assay down to 200 nM [56]. Except for cofactors detection, a ligase-regulated DNAzyme system was similarly developed to probe DNA ligase

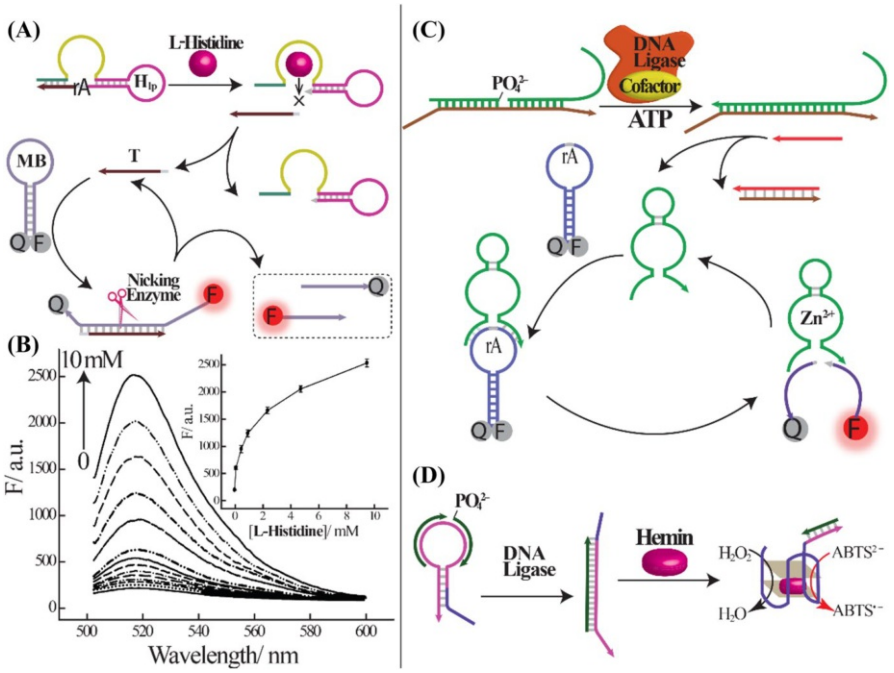

Fig. 12 **a** Schematic illustration of the cascade from L-Histidine-DNAzyme to nicking enzyme biocatalysis. **b** Fluorescence monitoring of the cascade DNAzyme system for histidine detection. Inset: Derived calibration curve. Reprinted with permission from Ref. [56]. Copyright 2011 American Chemical Society. **c** Schematic illustration of a coupled ligase/DNAzyme cascade for ATP detection. Reprinted with permission from Ref. [57]. Copyright 2011 American Chemical Society. **d** Schematic illustration of a coupled ligase/hemin/G-quadruplex for detecting ligase activity

activity [57]. One of the feasible examples is based on an allosteric DNAzyme-containing hairpin probe (HDP). With the help of DNA ligase, DNAzymes could be synthesized as "products" to achieve a more sensitive bioassay. As illustrated in Fig. 12c, the ligase-mediated ligation of two DNAzyme fragments activate the assembly of new DNAzyme. Only with ATP, then the ligase is active to assemble a new DNAzyme for cleaving the F/Q-labeled substrate, resulting in the generation of a high fluorescence signal. In another study, the DNAzyme domain is partially caged on the stem domain of a hairpin, Fig. 12d. [58]. Once the ligase repairs the nicking site and forms a more stable duplex DNA, then the hemin/G-quadruplex DNAzyme could be activated with peroxidase-like activity.

2.4 Integration

These catalytic CHA, cross-hybridization-involved HCR, and functional DNAzyme have shown great performance for amplified biosensing, yet are constrained with low signal gain. To make full use of these different enzyme-free circuits, the sophisticated cascading integration of these amplifiers was proposed to realize a

more readily quantitative detection as well as the assembly of exquisite DNA nanostructures [1]. Only through the corrected executions of individual reaction pathways, then the integrated multiple or cross-initiated enzyme-free amplifiers could be engineered for precisely detecting both nucleic acids and other analytes, leading to a higher amplification efficiency with delicate hierarchical DNA nanostructures [59]. The catalyzed translation of CHA leads to the assembly of numerous dsDNA by the preceding initiator.

For cascaded integration of catalytic hairpin assembly (CHA), the two-layered and three-layered CHA reactions have been engineered to further improve the signal amplification [60]. The integration depth of CHA was further promoted by using a cross-catalytic hairpin assembly (cross-CHA) circuit that consists of three CHA units, CHA-1, CHA-2, and CHA-3 (Fig. 13) [14]. Here, CHA-1 is composed of two hairpins H_A and H_B, which is initiated by trigger T to realize the assembly of H_A–H_B duplex through the catalyzed hairpin hybridization. The newly exposed single-stranded initiator of duplex H_A–H_B product can catalyze CHA-2 to assemble the H_C–H_D duplex from H_C and H_D reactants. Interestingly, the single-stranded region of duplex H_C–H_D is encoded with the same initiator sequence I that can reversely activate CHA-1 to generate another catalytic circuit "CHA-3". Therefore, the CHA-1 and CHA-2 circuits could mutually trigger each other by the intermediator "CHA-3" circuit, yielding an autocatalytic module for substantially promoting the cross-CHA-mediated exponential amplification.

The exposed single-stranded tether of CHA product could be utilized as a versatile trigger for motivating other DNA circuit, e.g., HCR circuit for generating long dsDNA polymers [61–64]. As shown in Fig. 14, the upstream catalytic CHA generates numerous dsDNA structures that each is decorated with an analogous sequence of T trigger for downstream HCR circuit. During this process, the low amount of

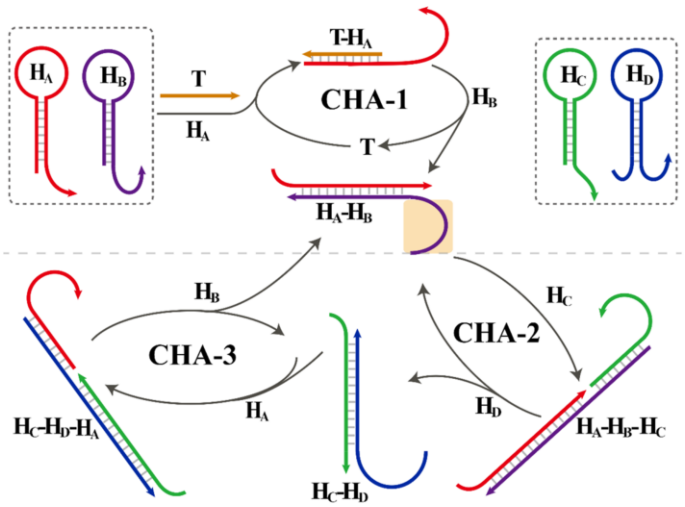

Fig. 13 Schematic illustration of the trigger T-driven cross-CHA circuit for yielding an exponential signal amplification

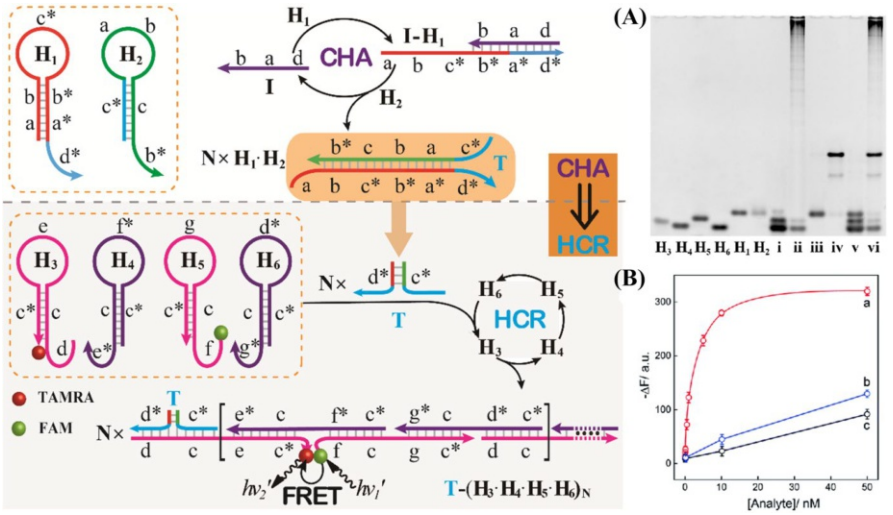

Fig. 14 Schematic illustration of the CHA–HCR system; **a** Gel–PAGE demonstration of the feasibility of CHA–HCR strategy: i/ii for HCR without/with T; iii/iv for CHA without/with I; v/vi for intact CHA-HCR without/with I. **b** Different calibration curves: (a) CHA–HCR, (b) HCR, and (c) CHA methods for analyzing different concentrations of analytes. Reprinted with permission from Ref. [65]. Copyright 2018 Royal Society of Chemistry

initiator **I** is transduced with the assembly of numerous duplex H_1–H_2 products, of which the newly exposed trigger T motivates the downstream HCR-driven sequential cross-hybridization among H_3, H_4, H_5, and H_6. This leads to the efficient assembly of plenty of long dsDNA copolymeric nanowires with the CHA trigger than that of HCR initiator (Fig. 14a). Then the respective FAM and TAMRA fluorophores of H_3 and H_5 are brought into close proximity, yielding a remarkably FRET signal [65]. This successive cascade hybridization between CHA and HCR realizes a sensitive detection of analytes. As shown in Fig. 14b, the CHA–HCR system showed a higher sensing-performance than the conventional CHA or HCR system, generating a significant synergistic amplification capacity.

The CHA circuit could also be translated into the assembly of DNAzyme catalyst. The integrated CHA–DNAzyme circuits showed great potential in high-performance biosensing applications [66, 67]. The sequential amplification feature of CHA–DNAzyme circuit could be further improved by using a cyclic-catalytic CHA–DNAzyme circuit where the DNAzyme biocatalysis could also trigger the initial CHA circuit (Fig. 15a) [68]. In the initial CHA scheme, initiator T catalyzes the cross-hybridization between H_1 and the fluorophore donor/acceptor-bearing H_2, yielding a ‘‘turn-on’’ fluorescence readout. The as-achieved H_1–H_2 duplex product carries an active DNAzyme that can cleave the T-caged S–L substrates to generate new trigger strands for reversely initiating the CHA circuit. Based on the programmable and modular characteristics, the cross-catalytic CHA–DNAzyme method is decomposed into two simplified basic reaction pathways, which are verified by theoretical simulations and experimental demonstrations (Fig. 15b, c, respectively).

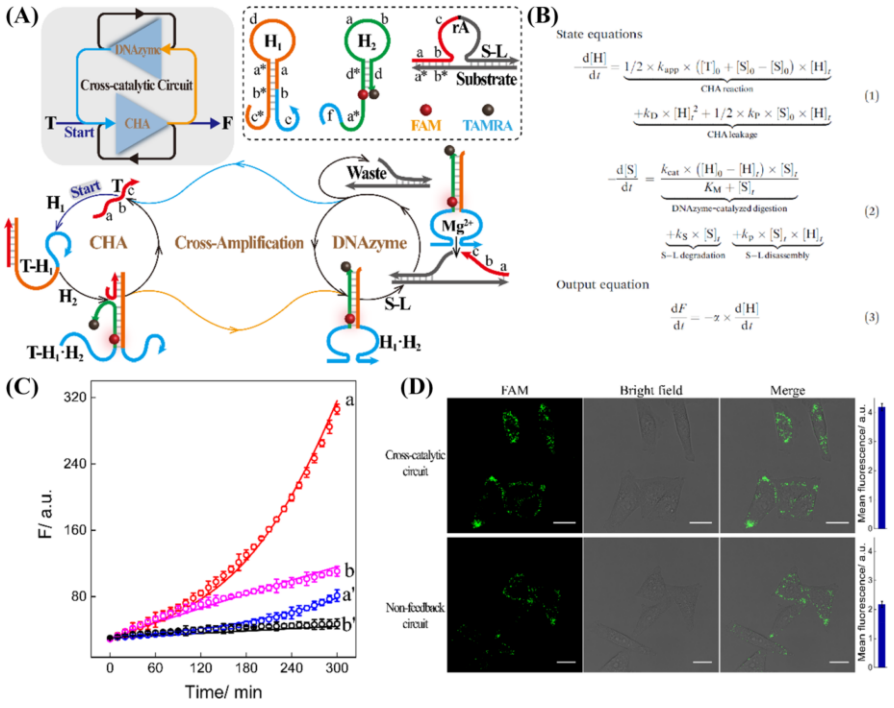

Fig. 15 Schematic illustration of the cross-catalytic CHA–DNAzyme circuit. **b** The mathematical model for cross-catalytic CHA–DNAzyme reaction simulation. **c** The fluorescence changes (solid lines represent for simulation results while circle dots represent for experimental data) of the cross-catalytic (a/a′) and non-feedback systems (b/b′) with/without input. Error bars ±SD ($n=3$). **d** CLSM imaging of miRNA in MCF-7 cells with the cross-catalytic and non-feedback-catalytic CHA–DNAzyme methods. Scale bars 20 μm. Reprinted with permission from Ref. [68]. Copyright 2019 Royal Society of Chemistry

Through the feedback DNAzyme loop, the newly exposed CHA initiators can essentially promote the assembly of numerous CHA products with high fluorescence readout. This isothermal cross-catalytic DNA circuit was then utilized as a general sensing strategy for amplified intracellular imaging of microRNA in living cells, which revealed a tremendously higher fluorescence readout than the conventional CHA–DNAzyme cascade (Fig. 15d).

Similarly, by precise design, the triple-layered CHA–HCR–DNAzyme circuit can also be integrated for amplified biosensing [61]. This isothermal autonomous enzyme-free DNA circuit system is constructed from the sequential integration of CHA, HCR, and DNAzyme amplifiers (Fig. 16a) [69]. The analyte-triggered CHA amplifier leads to the assembly of numerous dsDNA products in the first amplification stage. Here, the dsDNA products are encoded with HCR trigger sequence that can stimulate the cross-hybridization of HCR hairpins. Along with the generation of HCR copolymers, the DNAzyme biocatalysts are simultaneously activated for sustainably cleaving its fluorophore/quencher-labeled DNAzyme substrates, yielding an

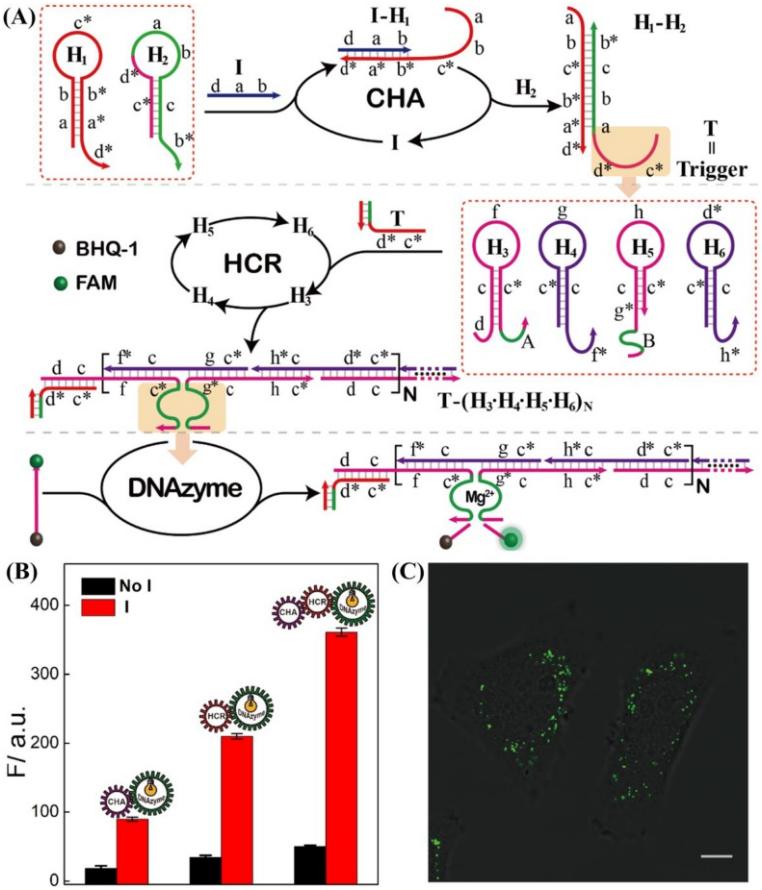

Fig. 16 **a** Scheme of the CHA–HCR–DNAzyme circuit. **b** The fluorescence monitoring the dual or triple DNA circuits initiated by their corresponding analytes. **c** Confocal imaging of miR-21 in MCF-7 cells through the CHA–HCR–DNAzyme system. Scale bar: 20 μm. Reprinted with permission from Ref. [69]. Copyright 2019 Royal Society of Chemistry

amplified fluorescence readout. As shown in Fig. 16b, the triple CHA–HCR–DNAzyme strategy realizes a more synergistic amplification performance than the dual CHA–DNAzyme and HCR–DNAzyme control circuits. This system was facilely introduced into living cells for intracellular imaging of microRNA with high signal gain and accuracy (Fig. 16c). Furthermore, the HRP-mimicking DNAzyme has also integrated with a cross-CHA circuit for amplified DNA detection with increased sensing performance by three orders of magnitude than traditional CHA [70].

As mentioned before, the HCR circuit could be heterogeneously integrated with a different CHA system. In fact, the HCR could also be integrated with a homologous HCR system to construct a cascade HCR system, where the initial HCR copolymer product could be elongated with new functional DNA branches through a sequential hybridization reaction [71]. The two-layered enzyme-free C-HCR circuit

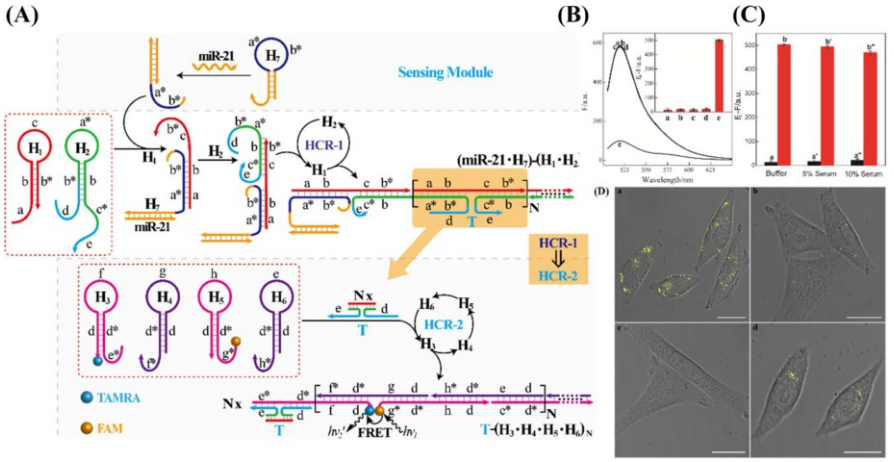

Fig. 17 Schematic illustration of the cascaded HCR circuit with a miR-21 sensing module. **b** Specific detection with the cascaded HCR system: a-e for no analyte, β-actin mRNA, let-7a, son DNA, and miR-21, respectively. Inset: summary of these fluorescence intensity readout. **c** The stability study of cascaded HCR-mediated miR-21 sensing system in serum buffer. bd Confocal imaging of miR-21 with FRET transduction (in the form of F_A/F_D) in (a/d) MCF-7/Hela cells by cascaded HCR amplifier, (b) MCF-7 cells by conventional HCR amplifier and (c) miR-21-inhibited MCF-7 cells by cascaded HCR amplifier. Scale bars 20 μm. Reprinted with permission from Ref. [72]. Copyright 2018 Royal Society of Chemistry

is composed of HCR-1 and HCR-2 circuits, which allows the first HCR-1 layer to be cascaded into the other HCR-2 circuit as shown in Fig. 17a [72]. Without initiator I, all hairpin reactants coexist metastable in the initial state. The initiator I triggers the successive cross-hybridization reaction between hairpins H_1 and H_2 in upstream HCR-1 for generating long dsDNA HCR-1 nanowires that concomitantly assemble the tandem trigger T. Here, the system realizes the first amplification stage by converting the limited amount of initiator into thousands of triggers through the successful cross-hybridization of upstream HCR-1. Subsequently, the newly generated T triggers HCR-2 to assemble dsDNA copolymers in the as-achieved HCR-1 DNA nanowires, where the fluorophore donor/acceptor pair is brought into close proximity for enabling the FRET process. This two-layered C-HCR circuit realizes a remarkably effective detection of microRNA with an improved anti-interference ability (Fig. 17b, c). Meanwhile, this amplification strategy has been further applied for miR-21 detection in living cells by coupling with a "plug-and-play" sensing module, whose promoted signal amplification capacity was demonstrated as compared with the conventional HCR system (Fig. 17d).

The facile design of HCR facilitates the assembly of tandem colocalized DNA sequences with more different decorations, e.g., DNAzymes. The HCR–DNAzyme amplification paradigm introduced a sensitive HCR-assembled DNAzyme amplification platform, Fig. 18a [73]. The HCR scheme is merely composed of two hairpins, which are grafted with two split functional DNAzyme subunits. The split DNAzyme stays in a catalytic inactive state for the absence of a favorable DNAzyme microenvironment. Once the analyte induces the assembly of two hairpins into dsDNA

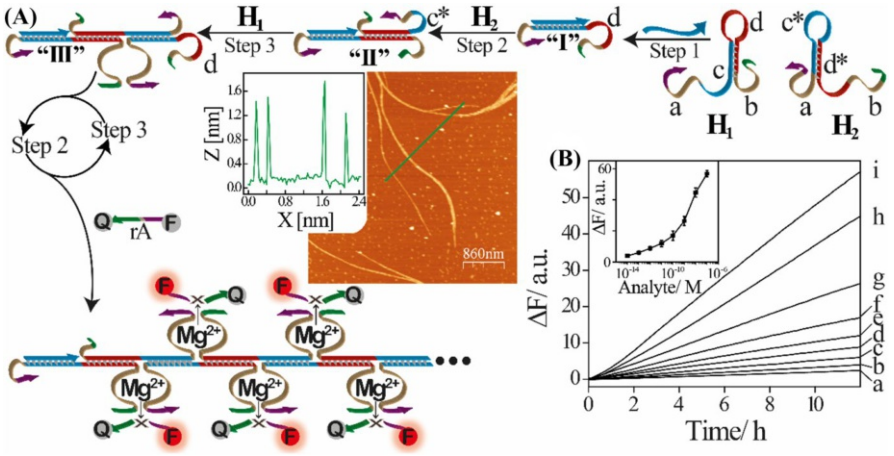

Fig. 18 **a** Schematic illustration of the HCR–DNAzyme cascade. Inset: AFM characterization of HCR copolymer nanowires. **b** Dynamic fluorescence changes of the HCR–DNAzyme system for detecting target with different concentrations: a–i for 0, 1×10^{-14}, 1×10^{-13}, 1×10^{-12}, 1×10^{-11}, 1×10^{-10}, 1×10^{-9}, 4×10^{-8}, and 2×10^{-7} M, respectively. Inset: Derived calibration curve. Reprinted with permission from Ref. [73]. Copyright 2011 American Chemical Society

polymer nanowires, the split DNAzyme subunits would be brought into close proximity on the HCR backbone, resulting in the assembly of a compact tandem DNAzyme nanostructures. These DNAzymes would be activated in the presence of their corresponding cofactors, leading to the cyclic cleavage of the F/Q-labeled DNAzyme substrate with a tremendously amplified fluorescence readout (Fig. 18b).

Many excellent systems have shown the merits of the cascade sensing features of synergistic HCRs, and sensitive HCR–DNAzyme systems [74]. Similarly, these previous cascaded HCR systems could also be integrated with the DNAzyme biocatalysis amplifier, Fig. 19a [75]. This triple-layered cascaded HCR–DNAzyme circuit is designed in a more compact and precise format. In the presence of an initiator, the preceding HCR-1 produces numerous analogous sequence T to motivate the following HCR-2, which concomitantly promotes the assembly of numerous tandem DNAzyme biocatalysts on the HCR-2 copolymer backbone. As demonstrated by AFM, large amounts of linear dsDNA copolymers are observed for the initiator-triggered HCR-1 system (Fig. 19b). As anticipated, micrometer-long dsDNA branches were observed after the initiation of CHCR–DNAzyme process with a height of ~ 2 nm. By incorporating a flexibly sensing module, this sophisticated CHCR–DNAzyme system extends its broad application for miRNAs detection in EVs.

Besides these different DNA hybridization networks, the varied DNAzymes could also be integrated for amplified sensing applications. As functional catalytic DNA strands, DNAzymes require the involvement of cofactors for executing an efficient biocatalysis and signal transduction. This property could be utilized for sensitively and selectively analyzing their corresponding cofactors by using the different DNAzyme or cascade DNAzyme systems. For example, the Pb^{2+}- or L-histidine-dependent DNAzyme could be initially applied to activate the assembly of two

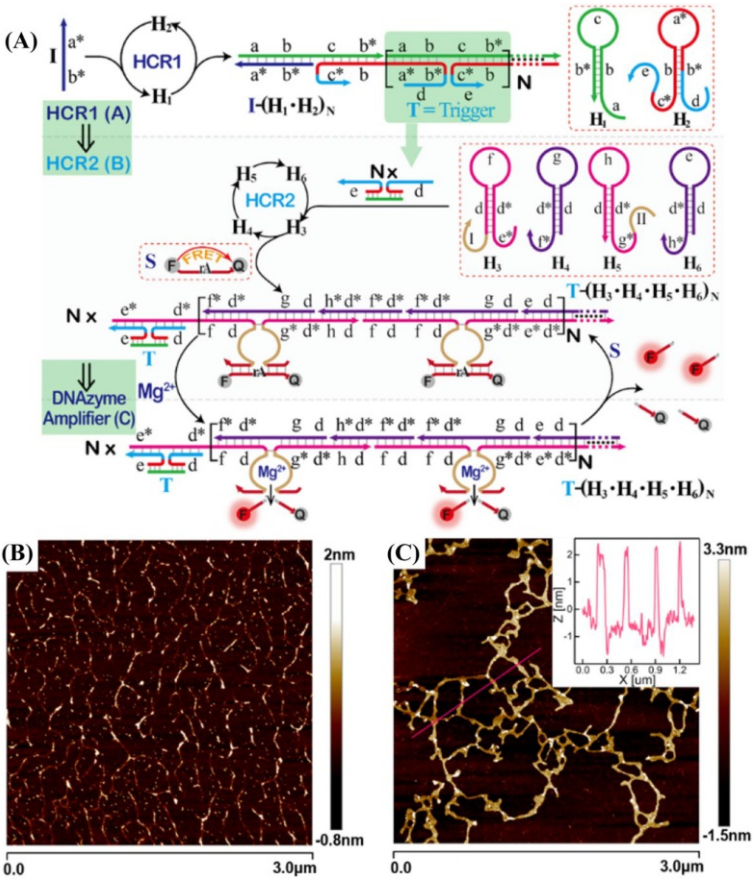

Fig. 19 **a** Schematic illustration of the cascade HCR–DNAzyme strategy. **b** AFM images of the HCR-1-assembled linear dsDNA polymers and **c** the cascade HCR-assembled branched dsDNA products. Reprinted with permission from Ref. [75]. Copyright 2019 American Chemical Society

hemin/G-quadruplex HRP-mimicking DNAzyme through the catalyzed disassembly of two cooperatively stabilized duplexes (Fig. 20a). Only with their corresponding cofactors, the DNAzyme substrate could be cleaved for releasing the hemin/G-quadruplex DNAzyme that enabled the colorimetric or chemiluminescence detection of Pb^{2+} or L-histidine (Fig. 20b, c) [76]. Here, the compact DNAzyme could be easily reconfigured into other metal ions or amino acid-dependent DNAzyme sequences, e.g., Pb^{2+}–DNAzyme (Fig. 20d), thus providing a universal and facile toolbox for more different bioassays.

DNAzymes also show great sensing performance through regenerating the target initiator by themselves [77], Fig. 21a. The autocatalytic DNAzyme system consists of two caged DNAzyme subunits and an initiator sequence-containing hairpin, which is functionalized with a F/Q pair in the stem's ends and a ribonucleobase (rA) in the loop. Target DNA induces the assembly of an

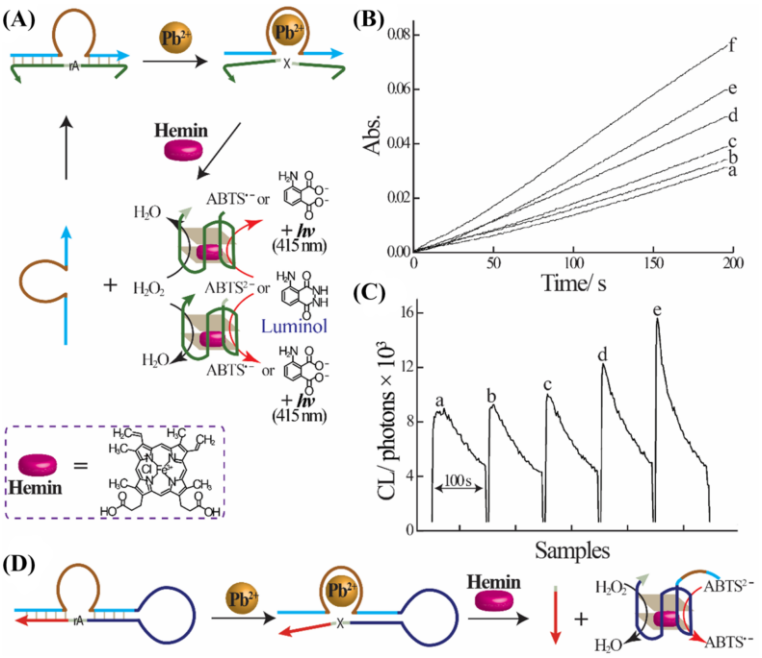

Fig. 20 **a** Schematic illustration of the cascade DNAzyme-(HRP) DNAzyme circuit for Pb^{2+} ions detection. **b** Absorbance and **c** chemiluminescence behaviors of DNAzyme cascade circuit for Pb^{2+} ions detection: a–f for 0, 1×10^{-8}, 1×10^{-7}, 5×10^{-7}, 1×10^{-6}, and 1×10^{-5} M, respectively. Reprinted with permission from Ref. [76]. Copyright 2008 Royal Society of Chemistry. **d** Schematic illustration of the cascade DNAzyme-(HRP) DNAzyme circuit with one compact DNA nanoprobe

inactive DNAzyme to specifically cleave the functional hairpin substrate with an enhanced fluorescence readout. Meanwhile, the cleaved fragment contains the same sequence of target DNA, thus inducing the initial assembly of DNAzymes for capturing and cleaving the substrate. Based on this catabolic replication method, this isothermal regenerating DNAzyme system realizes a significant signal amplification. Here, the RNA-cleaving DNAzyme could be replaced with a ligation DNAzyme, resulting in the assembly of an enzyme-free self-replication DNAzyme machinery. This cascade ligation DNAzyme was developed for detecting analyte, Fig. 21b [78]. Herein, target DNA hybridizes with the caged DNAzyme primer for generating a high fluorescence output and a new catalytic active ligation DNAzyme unit. With Zn^{2+}-cofactor, the ligation DNAzyme catalyzes the ligation of two fragments to form a similar strand of target DNA. The newly assembled target could be utilized for realizing ultrasensitive target DNA detection with the catalyzed assembly of more DNAzyme units.

In general, by taking advantage of these different amplification means, various integrated isothermal amplification strategies have provided more possibilities for realizing the more sensitive and selective detection of different analytes. These cascade DNA circuits could be considered as general amplification modules and

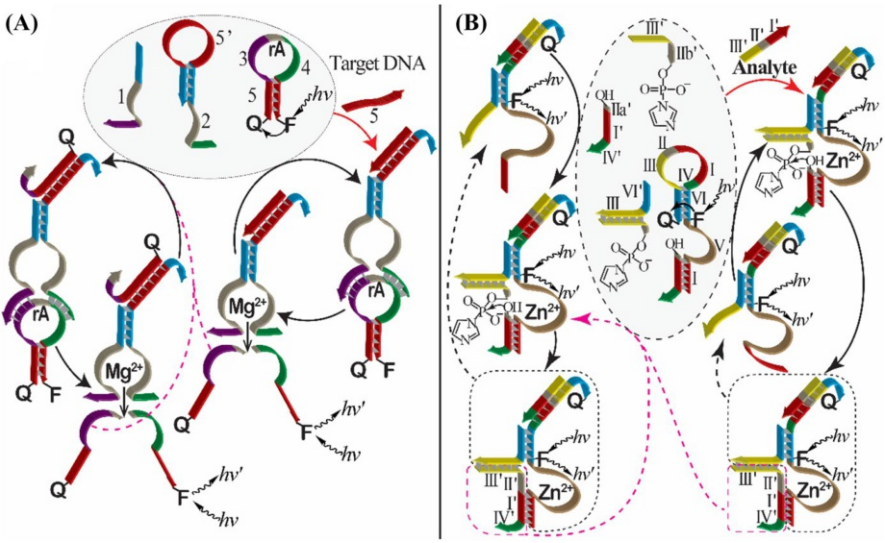

Fig. 21 **a** Scheme of the autocatalytic DNAzyme system based on the catabolic DNAzyme reaction. Reprinted with permission from Ref. [77]. Copyright 2011 Wiley–VCH. **b** Schematic illustration of a ligation DNAzyme-mediated replication DNAzyme machinery circuit. Reprinted with permission from Ref. [78]. Copyright 2012 American Chemical Society

further applied to parallelly detect various biomarkers with the help of other recognition elements, for example, aptamers [79], methylation [80, 81], uracil-DNA glycosylase [82], and special recognition sequence, e.g., C–Ag–C [83] or T–Hg–T [84] bridge. It is also interesting to develop a parallel analysis for more different targets with one cascaded catalytic machinery. In cells, the catalytic circuitry-based logic gates also contribute to the accurate analysis of more different biologically important targets in a complicated environment [85, 86]. The cascade DNA circuits could be applied for stimulating other signal transfer and complex signaling pathways that are involved with selective branching and feedback mechanisms, which can facilitate an in-depth and comprehensive understanding about the magical nature of living entities.

3 Conclusions and Future Perspectives

This chapter has discussed the different autonomous enzyme-free DNA circuits, including, catalytic hairpin assembly (CHA), hybridization chain reaction (HCR), catalytic functional nucleic acids (DNAzymes), and the integrated DNA reaction circuits in solution or on different nanoscaffolds (DNA, GOs [87] and AuNPs [88]). Based on the Watson–Crick base pairing, these enzyme-free amplification techniques have been successfully introduced for imaging intracellular mRNA [89, 90] or microRNA [91–94], and some interesting works also reported on surface-confined HCR on cells surface by the specific aptamer recognizing element (e.g.,

sgc8 aptamer binding PTK protein) with tremendously amplified transductions [95, 96]. Meanwhile, CHA, HCR, and DNAzyme could be integrated into a versatile and powerful toolbox with special functions through the cascade reaction format, which is especially suitable for isothermal conditions without special enzymes. Moreover, most of these circuits have been implemented in serum biological environments after a moderate modification of these DNA probes. The integration of DNA circuits could achieve improved sensitivity and selectivity for sensing applications in living entities. It is expected that these methods can be implemented with multiple sensing transductions, and show extensive potential for clinical diagnosis and prognosis.

Despite this progress, several challenges are still ahead of us. It is more appealing to realize intracellular analysis and to construct portable devices for POCT-based diagnosis, even though some commercial products have emerged. The intracellular amplified analyses of mRNA or microRNA are developed and non-nucleic acid biomolecules could also be converted into nucleic acid amplification events by introducing more configurable sensing modules [97]. Yet these systems are still confronted with more challenges, e.g., fragile and easy disturbance by the complicate bio-environment despite with relatively high stability. They are vulnerable to nonspecific adsorption and degradation in living animals. Single-layered enzyme-free circuits are relatively easy to be delivered into living cells by nanoparticles while cascade DNA circuits are more sophisticated with more DNA participants. This requires more efficient carriers to protect and transfer DNA primers to target tissues and cells. The specific and targeted delivery of DNA probes also represents a great challenge, so that the sophisticate DNA circuits could realize their functions as expected. What's more, all the reactants of DNA circuits need longer sensing durations. A promising route might be the utilization of intracellular cicerone to deliver them so that they can accumulate on a specific bio-compartments in a more efficient way. At the same time, some alternative nanomaterials could be introduced to ensure the proportional delivery of DNA probes and DNAzyme cofactors for DNAzyme-involved DNA reaction circuits.

Furthermore, based on the corrected executions of individual pathways, the autonomous DNA circuits have more significantly scientific implications far beyond biosensing. They might yield new properties and functions for the integration of diagnosis and immediate therapy. For example, the conjugation of gene-silencing functional DNAzyme with CHA or HCR can construct multiplexed catalytic DNA circuits with dual functions of sensing and disease treatment [98]. What's more, short-interfering RNAs are well developed to suppress gene expressions through a highly regulated enzyme-mediated process [99]. It is also a promising strategy to conjugate autonomous programmed cascade DNA circuits with siRNAs operations. In general, there is still much room for autonomous DNA circuits to implement. We hope this chapter will provide an overview of the autonomous enzyme-free DNA circuits for readers and inspire their interest to develop more strategies and discoveries in this interesting research field.

Acknowledgements This work is supported by National Natural Science Foundation of China (no. 21874103), National Basic Research Program of China (973 Program, 2015CB932601), and Fundamental Research Funds for the Central Universities (nos. 2042018kf0210 and 2042019kf0206).

References

1. Wang F-A, Lu CH, Willner I (2014) From cascaded catalytic nucleic acids to enzyme-DNA nanostructures: controlling reactivity, sensing, logic operations, and assembly of complex structures. Chem Rev 114:2881–2941
2. Lam B, Das J, Holmes RD, Live L, Sage A, Sargent EH, Kelley SO (2013) Solution-based circuits enable rapid and multiplexed pathogen detection. Nat Commun 4:2001
3. Benenson Y, Gil B, Ben-Dor U, Adar R, Shapiro E (2004) An autonomous molecular computer for logical control of gene expression. Nature 429:423–429
4. Maojo V, Martin-Sanchez F, Kulikowski C, Rodriguez-Paton A, Fritts M (2010) Nanoinformatics and DNA-based computing: catalyzing nanomedicine. Pediatr Res 67:481–489
5. Jo M, Ahn JY, Lee J, Lee S, Hong SW, Yoo JW, Kang J, Dua P, Lee DK, Hong S, Kim S (2011) Development of single-stranded DNA aptamers for specific bisphenol A detection. Oligonucleotides 21:85–91
6. Edwards K, Johnstone C, Thompson C (1991) A simple and rapid method for the preparation of plant genomic DNA for PCR analysis. Nucleic Acids Res 19:1349
7. Livak KJ, Schmittgen TD (2001) Analysis of relative gene expression data using real-time quantitative PCR and the 2(t)(-delta delta c) method. Methods 25:402–408
8. Tomita N, Mori Y, Kanda H, Notomi T (2008) Loop-mediated isothermal amplification (lamp) of gene sequences and simple visual detection of products. Nat Protoc 3:877–882
9. Wang J, Wang HM, Wang H, He SZ, Li RM, Deng Z, Liu XQ, Wang F-A (2019) Nonviolent self-catabolic DNAzyme nanosponges for smart anticancer drug delivery. ACS Nano 13:5852–5863
10. Zhang LR, Zhu GC, Zhang CY (2014) Homogeneous and label-free detection of microRNAs using bifunctional strand displacement amplification-mediated hyperbranched rolling circle amplification. Anal Chem 86:6703–6709
11. Walker GT, Fraiser MS, Schram JL, Little MC, Nadeau JG, Malinowski DP (1992) Strand displacement amplification—an isothermal, in vitro DNA amplification technique. Nucleic Acids Res 20:1691–1696
12. Zhou WH, Hu L, Ying LM, Zhao Z, Chu PK, Yu XF (2018) A CRISPR-cas9-triggered strand displacement amplification method for ultrasensitive DNA detection. Nat Commun 9:5012
13. Zhao YX, Chen F, Li Q, Wang LH, Fan CH (2015) Isothermal amplification of nucleic acids. Chem Rev 115:12491–12545
14. Yin P, Choi HM, Calvert CR, Pierce NA (2008) Programming biomolecular self-assembly pathways. Nature 451:318–322
15. Dirks RM, Pierce NA (2004) Triggered amplification by hybridization chain reaction. Proc Natl Acad Sci USA 101:15275–15278
16. Lai W, Xiong XW, Wang F, Li Q, Li L, Fan CH, Pei H (2019) Nonlinear regulation of enzyme-free DNA circuitry with ultrasensitive switches. ACS Synth Biol 8:2106–2112
17. Zhang DY, Winfree E (2009) Control of DNA strand displacement kinetics using toehold exchange. J Am Chem Soc 131:17303–17314
18. Xuan F, Hsing IM (2014) Triggering hairpin-free chain-branching growth of fluorescent DNA dendrimers for nonlinear hybridization chain reaction. J Am Chem Soc 136:9810–9813
19. Ying ZM, Wu Z, Tu B, Tan WH, Jiang JH (2017) Genetically encoded fluorescent RNA sensor for ratiometric imaging of microRNA in living tumor cells. J Am Chem Soc 139:9779–9782
20. Zhang KY, Song ST, Huang S, Yang L, Min QH, Wu XC, Lu F, Zhu JJ (2018) Lighting up microRNA in living cells by the disassembly of lock-like DNA-programmed UCNPS-AUNPS through the target cycling amplification strategy. Small 14:1802292–1802302
21. Zhang B, Liu BQ, Tang DP, Niessner R, Chen G, Knopp D (2012) DNA-based hybridization chain reaction for amplified bioelectronic signal and ultrasensitive detection of proteins. Anal Chem 84:5392–5399
22. Zhou YJ, Yang L, Wei J, Ma K, Gong X, Shang JH, Yu SS, Wang F-A (2019) An autonomous nonenzymatic concatenated DNA circuit for amplified imaging of intracellular ATP. Anal Chem 91:15229–15234
23. Liu NN, Hou RZ, Gao PC, Lou XD, Xia F (2016) Sensitive Zn^{2+} sensor based on biofunctionalized nanopores via combination of DNAzyme and DNA supersandwich structures. Analyst 141:3626–3629

24. Deng Y, Nie J, Zhang XH, Zhao MZ, Zhou YL, Zhang XX (2014) Hybridization chain reaction-based fluorescence immunoassay using DNA intercalating dye for signal readout. Analyst 139:3378–3383
25. Pan M, Liang M, Sun JL, Liu XQ, Wang F-A (2018) Lighting up fluorescent silver clusters via target-catalyzed hairpin assembly for amplified biosensing. Langmuir 34:14851–14857
26. Quan K, Huang J, Yang XH, Yang YJ, Ying L, Wang H, He Y, Wang KM (2015) An enzyme-free and amplified colorimetric detection strategy via target-aptamer binding triggered catalyzed hairpin assembly. Chem Commun 51:937–940
27. Jo EJ, Mun H, Kim SJ, Shim WB, Kim MG (2016) Detection of ochratoxin a (OTA) in coffee using chemiluminescence resonance energy transfer (CRET) aptasensor. Food Chem 194:1102–1107
28. Liang MJ, Pan M, Hu JL, Wang F-A, Liu XQ (2018) Electrochemical biosensor for microRNA detection based on cascade hybridization chain reaction. Chemelectrochem 5:1380–1386
29. Li BL, Ellington AD, Chen X (2011) Rational, modular adaptation of enzyme-free DNA circuits to multiple detection methods. Nucleic Acids Res 39:e110
30. Zheng AX, Wang JR, Li J, Song XR, Chen GN, Yang HH (2012) Enzyme-free fluorescence aptasensor for amplification detection of human thrombin via target-catalyzed hairpin assembly. Biosens Bioeletron 36:217–221
31. Jung C, Allen PB, Ellington AD (2016) A stochastic DNA walker that traverses a microparticle surface. Nat Nanotechnol 11:157–163
32. Wu CC, Cansiz S, Zhang LQ, Teng I, Qiu LP, Li J, Liu Y, Zhou CS, Hu R, Zhang T, Cui C, Cui L, Tan WH (2015) A nonenzymatic hairpin DNA cascade reaction provides high signal gain of mRNA imaging inside live cells. J Am Chem Soc 137:4900–4903
33. He L, Lu DQ, Liang H, Xie S, Zhang XB, Liu QL, Yuan Q, Tan WH (2018) mRNA-initiated, three-dimensional DNA amplifier able to function inside living cells. J Am Chem Soc 140:258–263
34. Huang J, Wu YR, Chen Y, Zhu Z, Yang XH, Yang CY, Wang KM, Tan WH (2011) Pyrene-excimer probes based on the hybridization chain reaction for the detection of nucleic acids in complex biological fluids. Angew Chem Int Ed 50:401–404
35. Shi ZL, Zhang XF, Cheng R, Li BX, Jin Y (2016) Sensitive detection of intracellular RNA of human telomerase by using graphene oxide as a carrier to deliver the assembly element of hybridization chain reaction. Analyst 141:2727–2732
36. Li L, Feng J, Liu HY, Li QL, Tong LL, Tang B (2016) Two-color imaging of microRNA with enzyme-free signal amplification via hybridization chain reactions in living cells. Chem Sci 7:1940–1945
37. Liu P, Yang XH, Sun S, Wang Q, Wang KM, Huang J, Liu JB, He LL (2013) Enzyme-free colorimetric detection of DNA by using gold nanoparticles and hybridization chain reaction amplification. Anal Chem 85:7689–7695
38. Zou L, Li RM, Zhang MJ, Luo YW, Zhou N, Wang J, Ling LS (2017) A colorimetric sensing platform based upon recognizing hybridization chain reaction products with oligonucleotide modified gold nanoparticles through triplex formation. Nanoscale 9:1986–1992
39. Wu Z, Liu GQ, Yang XL, Jiang JH (2015) Electrostatic nucleic acid nanoassembly enables hybridization chain reaction in living cells for ultrasensitive mRNA imaging. J Am Chem Soc 137:6829–6836
40. Ren KW, Xu YF, Liu Y, Yang M, Ju HX (2018) A responsive "nano string light" for highly efficient mRNA imaging in living cells via accelerated DNA cascade reaction. ACS Nano 12:263–271
41. Breaker RR, Joyce GF (1994) A DNA enzyme that cleaves RNA. Chem Bio 1:223–229
42. Carmi N, Balkhi SR, Breaker RR (1998) Cleaving DNA with DNA. Proc Natl Acad Sci USA 95:2233–2237
43. Liu ZJ, Mei SHJ, Brennan JD, Li YF (2003) Assemblage of signaling DNA enzymes with intriguing metal-ion specificities and ph dependences. J Am Chem Soc 125:7539–7545
44. Liu JW, Lu Y (2007) Rational design of "turn-on" allosteric DNAzyme catalytic beacons for aqueous mercury ions with ultrahigh sensitivity and selectivity. Angew Chem Int Ed 46:7587–7590
45. Santoro SW, Joyce GF, Sakthivel K, Gramatikova S, Barbas CF (2000) RNA cleavage by a DNA enzyme with extended chemical functionality. J Am Chem Soc 122:2433–2439
46. Liang G, Man Y, Li A, Jin XX, Liu XH, Pan LG (2017) DNAzyme-based biosensor for detection of lead ion: a review. Microchem J 131:145–153
47. McGhee CE, Loh KY, Lu Y (2017) DNAzyme sensors for detection of metal ions in the environment and imaging them in living cells. Curr Opin In Biotech 45:191–201
48. Zhou WH, Saran R, Liu JW (2017) Metal sensing by DNA. Chem Rev 117:8272–8325

49. Li J, Lu Y (2000) A highly sensitive and selective catalytic DNA biosensor for lead ions. J Am Chem Soc 122:10466–10467
50. Golub E, Freeman R, Willner I (2011) A hemin/g-quadruplex acts as an NADH oxidase and NADH peroxidase mimicking DNAzyme. Angew Chem Int Ed 50:11710–11714
51. Pavlov V, Xiao Y, Gill R, Dishon A, Kotler M, Willner I (2004) Amplified chemiluminescence surface detection of DNA and telomerase activity using catalytic nucleic acid labels. Anal Chem 76:2152–2156
52. Li T, Shi LL, Wang EK, Dong SJ (2009) Silver-ion-mediated DNAzyme switch for the ultrasensitive and selective colorimetric detection of aqueous Ag + and cysteine. Chemistry 15:3347–3350
53. Liu JW, Lu Y (2003) A colorimetric lead biosensor using DNAzyme-directed assembly of gold nanoparticles. J Am Chem Soc 125:6642–6643
54. Yang YJ, Huang J, Yang XH, Quan K, Wang H, Ying L, Xie N, Ou M, Wang KM (2016) Aptazyme-gold nanoparticle sensor for amplified molecular probing in living cells. Anal Chem 88:5981–5987
55. Zhao XH, Kong RM, Zhang XB, Meng HM, Liu WN, Tan WH, Shen GL, Yu RQ (2011) Graphene-DNAzyme based biosensor for amplified fluorescence "turn-on" detection of Pb^{2+} with a high selectivity. Anal Chem 83:5062–5066
56. Kong RM, Zhang XB, Chen Z, Meng HM, Song ZL, Tan WH, Shen GL, Yu RQ (2011) Unimolecular catalytic DNA biosensor for amplified detection of L-histidine via an enzymatic recycling cleavage strategy. Anal Chem 83:7603–7607
57. Lu LM, Zhang XB, Kong RM, Yang B, Tan Wh (2011) A ligation-triggered DNAzyme cascade for amplified fluorescence detection of biological small molecules with zero-background signal. J Am Chem Soc 133:11686–11691
58. He KY, Li W, Nie Z, Huang Y, Liu ZL, Nie LH, Yao SZ (2012) Enzyme-regulated activation of DNAzyme: a novel strategy for a label-free colorimetric DNA ligase assay and ligase-based biosensing. Chemistry 18:3992–3999
59. Li BL, Jiang Y, Chen X, Ellington AD (2012) Probing spatial organization of DNA strands using enzyme-free hairpin assembly circuits. J Am Chem Soc 134:13918–13921
60. Dai JY, He HF, Duan ZJ, Guo Y, Xiao D (2017) Self-replicating catalyzed hairpin assembly for rapid signal amplification. Anal Chem 89:11971–11975
61. Feng CJ, Zhu J, Sun JW, Jiang W, Wang L (2015) Hairpin assembly circuit-based fluorescence cooperative amplification strategy for enzyme-free and label-free detection of small molecule. Talanta 143:101–106
62. Quan K, Huang J, Yang XH, Yang YJ, Ying L, Wang H, Xie NL, Ou M, Wang KM (2016) Powerful amplification cascades of FRET-based two-layer nonenzymatic nucleic acid circuits. Anal Chem 88:5857–5864
63. Wei YL, Zhou WJ, Li X, Chai YQ, Yuan R, Xiang Y (2016) Coupling hybridization chain reaction with catalytic hairpin assembly enables non-enzymatic and sensitive fluorescent detection of microRNA cancer biomarkers. Biosens Bioelectron 77:416–420
64. Wu XY, Chai YQ, Yuan R, Zhuo Y, Chen Y (2014) Dual signal amplification strategy for enzyme-free electrochemical detection of microRNAs. Sensors Actuators B-Chem 203:296–302
65. Wang HM, Li CX, Liu XQ, Zhou X, Wang F-A (2018) Construction of an enzyme-free concatenated DNA circuit for signal amplification and intracellular imaging. Chem Sci 9:5842–5849
66. Liu SF, Cheng CB, Gong HW, Wang L (2015) Programmable Mg^{2+}-dependent DNAzyme switch by the catalytic hairpin DNA assembly for dual-signal amplification toward homogeneous analysis of protein and DNA. Chem Commun 51:7364–7367
67. Yang L, Wu Q, Chen YQ, Liu XQ, Wang F-A, Zhou X (2019) Amplified microRNA detection and intracellular imaging based on an autonomous and catalytic assembly of DNAzyme. ACS Sens 4:110–117
68. Zou LN, Wu Q, Zhou YJ, Gong X, Liu XQ, Wang F-A (2019) A DNAzyme-powered cross-catalytic circuit for amplified intracellular imaging. Chem Commun 55:6519–6522
69. Wang H, Wang HM, Wu Q, Liang MJ, Liu XQ, Wang F-A (2019) A DNAzyme-amplified DNA circuit for highly accurate microRNA detection and intracellular imaging. Chem Sci 10:9597–9604
70. Yue SZ, Zhao TT, Qi HJ, Yan YC, Bi S (2017) Cross-catalytic hairpin assembly-based exponential signal amplification for CRET assay with low background noise. Biosens Bioelectron 94:671–676
71. Bi S, Chen M, Jia XQ, Dong Y, Wang ZH (2015) Hyperbranched hybridization chain reaction for triggered signal amplification and concatenated logic circuits. Angew Chem Int Ed 54:8144–8148

72. Wei J, Gong X, Wang Q, Pan M, Liu XQ, Liu J, Xia F, Wang F-A (2018) Construction of an autonomously concatenated hybridization chain reaction for signal amplification and intracellular imaging. Chem Sci 9:52–61
73. Wang F-A, Elbaz J, Orbach R, Magen N, Willner I (2011) Amplified analysis of DNA by the autonomous assembly of polymers consisting of DNAzyme wires. J Am Chem Soc 133:17149–17151
74. He DG, Hai L, Wang HZ, Wu R, Li HW (2018) Enzyme-free quantification of exosomal microRNA by the target-triggered assembly of the polymer DNAzyme nanostructure. Analyst 143:813–816
75. Wu Q, Wang H, Gong KK, Shang JH, Liu XQ, Wang F-A (2019) Construction of an autonomous nonlinear hybridization chain reaction for extracellular vesicles-associated microRNAs discrimination. Anal Chem 91:10172–10179
76. Elbaz J, Shlyahovsky B, Willner I (2008) A DNAzyme cascade for the amplified detection of pb(2+) ions or L-histidine. Chem Commun 13:1569–1571
77. Wang F-A, Elbaz J, Teller C, Willner I (2011) Amplified detection of DNA through an autocatalytic and catabolic DNAzyme-mediated process. Angew Chem Int Ed 50:295–299
78. Wang F-A, Elbaz J, Willner I (2012) Enzyme-free amplified detection of DNA by an autonomous ligation DNAzyme machinery. J Am Chem Soc 134:5504–5507
79. Zhang ZX, Sharon E, Freeman R, Liu XQ, Willner I (2012) Fluorescence detection of DNA, adenosine-5 '-triphosphate (ATP), and telomerase activity by zinc(ii)-protoporphyrin ix/g-quadruplex labels. Anal Chem 84:4789–4797
80. Li CX, Wang HM, Shang JH, Liu XQ, Yuan B, Wang F-A (2018) Highly sensitive assay of methyltransferase activity based on an autonomous concatenated DNA circuit. ACS Sens 3:2359–2366
81. Wang Q, Pan M, Wei J, Liu XQ, Wang F-A (2017) Evaluation of DNA methyltransferase activity and inhibition via isothermal enzyme-free concatenated hybridization chain reaction. ACS Sens 2:932–939
82. Wang J, Pan M, Wei J, Liu XQ, Wang F-A (2017) A C-HCR assembly of branched DNA nanostructures for amplified uracil-DNA glycosylase assays. Chem Commun 53:12878–12881
83. Liu L, Li Q, Tang LJ, Yu RQ, Jiang JH (2016) Silver nanocluster-lightened hybridization chain reaction. RSC Adv 6:57502–57506
84. Chen PP, Wu P, Zhang YX, Chen JB, Jiang XM, Zheng CB, Hou XD (2016) Strand displacement-induced enzyme-free amplification for label-free and separation-free ultrasensitive atomic fluorescence spectrometric detection of nucleic acids and proteins. Anal Chem 88:12386–12392
85. Gong X, Wei J, Liu J, Li RM, Liu XQ, Wang F-A (2019) Programmable intracellular DNA biocomputing circuits for reliable cell recognitions. Chem Sci 10:2989–2997
86. Orbach R, Willner B, Willner I (2015) Catalytic nucleic acids (DNAzymes) as functional units for logic gates and computing circuits: from basic principles to practical applications. Chem Commun 51:4144–4160
87. Hong C, Kim DM, Baek A, Chung H, Jung W, Kim DE (2015) Fluorescence-based detection of single-nucleotide changes in RNA using graphene oxide and DNAzyme. Chem Commun 51:5641–5644
88. Chen XP, Wang L, Sheng SC, Wang T, Yang J, Xie GM, Feng WL (2015) Coupling a universal DNA circuit with graphene sheets/polyaniline/AUNPS nanocomposites for the detection of BCR/ABL fusion gene. Anal Chim Acta 889:90–97
89. Huang J, Wang H, Yang XH, Quan K, Yang YJ, Ying L, Xie NL, Ou M, Wang KM (2016) Fluorescence resonance energy transfer-based hybridization chain reaction for in situ visualization of tumor-related mRNA. Chem Sci 7:3829–3835
90. Wang SF, Ding JS, Zhou WH (2019) An aptamer-tethered, DNAzyme-embedded molecular beacon for simultaneous detection and regulation of tumor-related genes in living cells. Analyst. 144:5098–5107
91. Bi S, Ye JY, Dong Y, Li HT, Cao W (2016) Target-triggered cascade recycling amplification for label-free detection of microRNA and molecular logic operations. Chem Commun 52:402–405
92. Deng RJ, Zhang KX, Li JH (2017) Isothermal amplification for microRNA detection: from the test tube to the cell. Accounts Chem Res 50:1059–1068
93. Wu H, Liu YL, Wang HY, Wu J, Zhu FF, Zou P (2016) Label-free and enzyme-free colorimetric detection of microRNA by catalyzed hairpin assembly coupled with hybridization chain reaction. Biosens Bioeletron 81:303–308
94. Yang L, Liu CH, Ren W, Li ZP (2012) Graphene surface-anchored fluorescence sensor for sensitive detection of microRNA coupled with enzyme-free signal amplification of hybridization chain reaction. ACS Appl Mater Interfaces 4:6450–6453

95. Chang X, Zhang C, Lv C, Sun Y, Zhang MZ, Zhao YM, Yang LL, Han D, Tan WH (2019) Construction of a multiple-aptamer-based DNA logic device on live cell membranes via associative toehold activation for accurate cancer cell identification. J Am Chem Soc 141:12738–12743
96. Yuan BY, Chen YY, Sun YQ, Guo QP, Huang J, Liu JB, Meng XX, Yang XH, Wen XH, Li ZH, Li L, Wang KM (2018) Enhanced imaging of specific cell-surface glycosylation based on multi-FRET. Anal Chem 90:6131–6137
97. Wu PW, Hwang KV, Lan T, Lu Y (2013) A DNAzyme-gold nanoparticle probe for uranyl ion in living cells. J Am Chem Soc 135:5254–5257
98. Feng J, Xu Z, Liu F, Zhao Y, Yu WQ, Pan M, Wang F-A, Liu XQ (2018) Versatile catalytic deoxyribozyme vehicles for multimodal imaging-guided efficient gene regulation and photothermal therapy. ACS Nano 12:12888–12901
99. Brummelkamp TR, Bernards R, Agami R (2002) A system for stable expression of short interfering RNAs in mammalian cells. Science 296:550–553